Biological Holography Mapped onto the Cosmos: Capsules, Black Holes and the Generational Inheritance of Universes

Guoxing Gu

*Independent Researcher, Edmonton, Alberta, Canada.
ORCID: 0009-0006-0118-806X.

Corresponding author(s). E-mail(s): guoxing.gu@oseeds.ca;

Abstract

Physics has developed dedicated theories of entropy, holography and information conservation for black holes alone, because a black hole alone compresses information to the capacity limit of its surface; if black holes give birth to new universes, the information retained at a burst can only be passed on to the next generation, which corresponds to the concentration of biological information in the cell nucleus and the germ cells. Building on four previous papers [1–4], we map biological holography to cosmic scales. Black-hole formation obeys a unified density criterion ρ_c/N^2, and the survival of early black holes is set by a critical mass. The event horizon and the Cauchy horizon correspond to the outer and inner nuclear membranes; the outer-horizon entropy corresponds to surface information and the inner-horizon entropy to bulk information; the spin $\chi = \sqrt{3}/2$ divides black holes into prokaryotic and eukaryotic types. A cosmic egg cell breaks in one step at the existence boundary and bursts, and the registrations on the two horizons of the parent black hole transfer to the Hubble sphere of our universe. The three evolutionary pathways of E_c correspond to dark energy, dark matter and visible matter. The CMB axis of evil, the Cold Spot and supermassive black holes may form an ancestral–parent–child "three generations in one frame" observational clue.

Keywords: Biological holography, Black-hole formation criterion, Primordial black holes, Dark-energy capsule, Black-hole burst, Transgenerational pre-setting

1 Introduction

An intriguing phenomenon is one of the starting points of this paper. The literature on black-hole entropy and black-hole information is vast: from the Bekenstein–Hawking entropy [5] and the holographic principle [6–8] to the conservation of black-hole information and the Page curve [3], "information is not lost in a black hole" has become a broad consensus. The unitarity of quantum mechanics holds for every physical system, and the Solar System and the Milky Way do not lose information either; yet no one has built a dedicated theory of entropy and holography for them. Physics concentrates the problem of information on black holes because only a black hole compresses information to the limit that its surface can hold, and only a black hole forces the question: where does the information that enters it go? If the view that black holes give birth to new universes holds [9], the question has a natural answer: the information still retained at a burst can neither disappear nor stay in the original black-hole structure, and can only be passed on to the next generation with the burst (Section 7.2). In living organisms, too, the storage and transmission of information are not shared evenly but are concentrated in the cell nucleus and the germ cells. It is this correspondence that leads us to map biological holography to cosmic scales.

The combination of the holographic principle with systemic recursion offers a new perspective for crossing the disciplinary barrier between microscopic biology and macroscopic astrophysics. Traditional physics often regards a black hole as a spacetime singularity and the end point of matter, while biology attributes the evolution and reproductive strategies of organisms to selection under local environmental pressure. If one sets aside the specific materials and scales and looks only at spatial geometric structure, informational phase transitions and system control, extreme celestial objects and biological units show a marked fractal self-similarity and organizational isomorphism.

The core argument of this paper is a hypothetical and exploratory structural mapping: organizing principles repeatedly verified in biological systems (the domain–boundary structure, the differentiation of germ cells from somatic cells, transgenerational pre-setting, biological holography and so on) are mapped to astrophysical scales. This is not a rigorous mathematical proof of the proposition that "the universe has a holographic structure", but the mapping provides an internally consistent and unified view of a series of seemingly unrelated questions: why dark matter does not take part in electromagnetic interactions; when and with what masses primordial black holes (PBHs) formed and survived to the present; whether celestial bodies contain black-hole cores; why the Cold Spot of the cosmic microwave background (CMB) and the anomalous alignment of its low multipoles coexist; and how dark energy, dark matter and visible matter (i.e. ordinary, baryonic matter) are related. The specific mechanisms proposed here on physical grounds often find independent, structurally corresponding precedents in biology, and this cross-disciplinary mutual support is the core value that the paper hopes to present. Where a point is disputed, we do not avoid the controversy: we present the opposing evidence faithfully, state our own position, and leave the verdict to observation and further work.

1.1 The four previous papers and the position of this paper

This paper builds on four previous papers; for definitions and derivations already given there, only the conclusions are quoted.

Unified Recursive Organization Theory [1] (hereafter Paper I) proposed the domain–boundary framework: every stable organization has both a bulk state and a surface state, corresponding to the bulk information potential Ψ_b and the surface information potential Ψ_s, and when the bulk has structure, information is stored mainly in the bulk; the formation of organization appears as a continuous process of structural recurrence and structural recursion; living systems maintain the continuity of organization by continuous recursive pre-setting of the initial source of organizational information, i.e. transgenerational germline pre-setting, rather than by reverse compression from the mature individual.

The $2d_m$ Minimum Topological Structural Unit [2] (hereafter Paper II) derived the $2d_m$ axiom from "information is the measure of distinguishable relations between objects" and constructed the dark-energy capsule unit E_c: inner diameter $D_i = 2\ell_p$, outer diameter $D_o = 4\ell_p$, energy E_P; the force balance of the spacetime interfacial tension gives the inner-interface radius ℓ_p of a capsule, and the outer interface lies exactly at the Schwarzschild radius $2\ell_p$ of E_P; full topological normalization resolves the vacuum-energy paradox, and the measured dark-energy density is interpreted as the residual potential $\delta_c\rho_c$, $\delta_c = \Omega_\Lambda/N_{\mathcal{H}}^2$, where Ω_Λ is the dark-energy density parameter (the ratio of the dark-energy density to the critical density) and $N_{\mathcal{H}} \approx 4.25 \times 10^{60}$ is the capsule count of the Hubble sphere.

Relational Structure of the Bekenstein–Hawking Entropy [3] (hereafter Paper III) took the capsule number N as the counting unit and gave the exact decomposition of black-hole entropy $S/k_B = 4\pi N^2 = 4\pi[N + N(N-1)]$: one self term per capsule and two ordered relations per pair of capsules; accretion and evaporation are quantized at two levels, in energy by whole packs of E_P and in area by sub-steps $A_o = 16\pi\ell_p^2$; the horizon accepts only unpacked energy, packing takes place at the inner interface R_i, and the relations are registered on the horizons; temperature matching requires unpacking to be last-in-first-out; the contact density required for two E_c to combine into the smallest black hole exists only in the early universe; in a merger a common outer interface encloses both, the smaller black hole dissolves while its capsule packs are absorbed as a whole and re-registered; the conservation of relational entropy gives the Page curve directly. For a Kerr black hole, the entropies of the two horizons are each obtained from their own areas: the outer horizon carries the irreducible part $4\pi k_B N_{irr}^2$, the inner horizon the rotational part, and their sum is $4\pi k_B N^2$; the difference of the areal radii of the two horizons is not smaller than $2\ell_p$, which constitutes the existence criterion for black holes.

Angular-Momentum Spectrum of Kerr Black Holes [4] (hereafter Paper IV) showed from the $2d_m$ axiom that the lower limit $2\ell_p$ of the existence criterion is the minimum distinguishable span, and gave the integer range of allowed states and the two-level angular-momentum spectrum: black holes with $N \leq 4$ cannot rotate, and the smallest rotating state is $BH(5, 4)$; the envelope of the spin upper limit, $\chi_{\max} = 1 - 1/N^2$, is the existence boundary, reached exactly only by integer states satisfying the Pell

equation, at which the separation of the two horizons is exactly $2\ell_p$; near the boundary the absorption of one rotational pack breaks the structure in one step, and the classical extremal point at which the two horizons coincide cannot be reached; the prokaryote/eukaryote division $\chi = \sqrt{3}/2$ cannot be occupied exactly by an integer state but can be crossed in one step.

The task of this paper is to place these four sets of results in a single cross-scale framework and to answer questions that the previous papers did not: how and when black holes form and whether they survive; how the interface structure of a black hole corresponds to a cell; whether celestial bodies have black-hole cores; how our universe is related to black holes; and how dark energy, dark matter and visible matter arise from a single process.

1.2 Controversies involved and the position of this paper

The argument of this paper rests on several questions on which there is genuine disagreement. The opposing evidence and our position are stated one by one below.

Dark matter and black holes. We take the physical entity of dark matter to be the whole population of black holes across all mass scales, from the smallest primordial black holes surviving to the present, through stellar-mass and intermediate-mass black holes, up to supermassive black holes of the TON 618 class. Black holes in non-accreting, non-merging phases are electromagnetically silent, in accordance with the property that dark matter "does not take part in electromagnetic interactions". It must be stated plainly that optical gravitational microlensing and other observations have excluded primordial black holes as all of the dark matter in several mass ranges [10], and that the mainstream more often considers non-baryonic candidates such as weakly interacting massive particles (WIMPs) and axions. Existing lensing constraints mostly assume a single characteristic mass; if the mass spectrum is extended, the densities summed over the windows may suffice to account for all the dark matter, but the extension into other windows may also violate the constraints there [11]. This disagreement is unresolved.

The formation mechanism of black holes. We hold that black-hole formation obeys a unified density criterion (Section 3.2): the density reaches the mean black-hole density corresponding to the number of capsules contained. Primordial black holes and stellar-collapse black holes differ only in when, and with what N, this criterion is satisfied, not in being two different physical mechanisms.

Dark energy. We adopt the conclusion of Paper II: dark energy is the residual potential of the background capsules; the capsules are created with the expansion at constant density, the residual coefficient δ_c is a constant, and the energy density does not dilute with the expansion, so that the equation of state is $w = -1$. Recent baryon-acoustic-oscillation observations by the Dark Energy Spectroscopic Instrument (DESI) suggest that $w(z)$ may evolve slowly with time [12, 13], but the statistical significance is limited and the result is not generally accepted; if the indication is confirmed, it will be a direct test of this paper and of Paper II.

Spatial clustering of primordial black holes. We hold that black holes, as basic organizational units of the universe, should be clustered like stars and galaxies. Clustering makes lensing paths overlap, so that surveys systematically underestimate

the abundance [14], and also makes primordial black holes more likely to merge in binaries, in agreement with the binary black-hole merger rate of LIGO–Virgo [15]. Studies taking the opposite view point out that clustering can at most relax, not evade, the lensing constraints [16], and that highly clustered initial primordial black holes would produce merger rates far above those observed [17]. We regard the core of the disagreement as the modelling of the degree and scale of clustering; the present evidence is insufficient to decide, and we adopt the former picture.

The status of Bohm's implicate order. We adopt the framework of the implicate and explicate orders [18, 19] and of the super-implicate order [20] proposed by Bohm. Bohm used it to describe the wholeness of the entire universe: the whole is enfolded in every part and unfolds in spacetime into visible objects and events. In the picture of this paper, a black hole is a universe not yet unfolded; the burst of a black hole into a new universe and the formation of celestial bodies in the new universe are both macroscopic transitions from the implicate to the explicate order, so the framework can be applied directly to black holes. Bohmian mechanics is not the mainstream among interpretations of quantum mechanics; what we adopt is its ontological position that "the whole is implicit in the unfolding of the parts", and in Section 5.5 we give its concrete meaning for black holes: the implicate and explicate orders are the internal and external readings of the same set of relations.

Cosmic generations and CMB anomalies. We regard our universe as the result of a parent black hole that was gestated in the ancestral universe and then burst, in line with Smolin's hypothesis of cosmological natural selection [9] (Section 4.6); we regard the CMB "axis of evil" as an imprint left by the ancestral universe and the Cold Spot as the remnant of the parent black hole (Section 6). The statistical significance and the origin of both anomalies are disputed, and we state this plainly.

1.3 Outline

Section 2 sets up the geometric language of the domain–boundary hierarchy and gives the interface structure of black holes, the distribution of information over the two horizons of a Kerr black hole, and the correspondence between black holes and prokaryotic/eukaryotic cells. Section 3 discusses E_c and black holes as two levels of basic units: the unified density criterion for black-hole formation, the conditions for formation and survival in the early universe, accretion and mergers, black-hole cores inside celestial bodies, and the mass spectrum, clustering and detection. Section 4 discusses cosmic egg cells, the parent black hole and its relation to our universe, and black-hole bursts, with a comparison with Smolin's hypothesis of cosmological natural selection. Section 5 unifies dark energy, dark matter and visible matter as the three evolutionary pathways of E_c and defines the implicate and explicate orders. Section 6 discusses CMB anomalies and "three generations in one frame". Section 7 discusses deconstruction, information conservation and the cross-scale mapping of three-level mechanisms of inheritance. Section 8 gives the conclusions, limitations and outlook.

2 Domain–boundary structure: from layered celestial bodies to black holes

2.1 Domain and boundary, and unified organizational information

Paper I [1] gave the full definition of the domain–boundary framework: every organizational domain has both a bulk state and a surface state, and the unified organizational information is

$$\Psi(D) = \Psi_b(D) + \Psi_s(D) \tag{1}$$

As shown in Fig. 1(a), the bulk information potential Ψ_b is responsible for the storage, inheritance and historical memory of information, and the surface information potential Ψ_s for recognition, exchange, coupling and the formation of new organization; when two organizational domains remain coupled, the nonlinear action of the surface information potentials forms a new coupling interface, which can grow further into a new organizational domain, so that the formation of organization is a continuous recursive process [1]. This division of labour presupposes that the bulk has structure. The cell nucleus contains complex structures such as chromatin made of DNA and histones, and information can be stored in the bulk. When the bulk loses the structures that can carry information, for example when matter is compressed into a black hole and only rest-massless energy packs (E_c) remain, the storage of information can only move to the surface, and the upper limit of organizational information is set by the surface area; this is the content of the holographic principle for black holes [5–8]. The black hole is the limit of this situation (see Section 2.4).

Paper I divided every organizational domain into manifest matter (mass and structure) and unmanifest information (energy and organizational code) [1]. To treat celestial scales, we add fields and rest-massless particles to unmanifest information and introduce between the two a transitional state: fields and elementary particles, which may include some massless particles. Manifest matter and unmanifest information convert into each other through the transitional state (Fig. 1(b)). When information corresponds to a particular organizational domain, it is called unified organizational information.

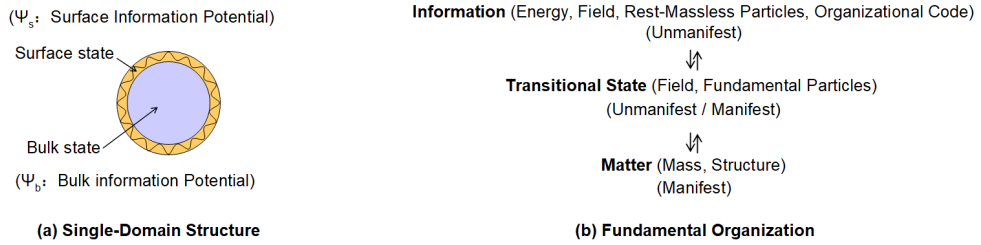

Fig. 1 Concepts of domain-boundary structure and fundamental organization

Information and matter are related quantitatively. For a bounded system of radius R and energy E, the amount of information (in bits) does not exceed $2\pi RE/(\hbar c \ln 2)$ [21]; a black hole attains this upper limit. Setting $E = Mc^2$ and $R = R_s = 2GM/c^2$ gives

$$I_{\mathrm{BH}} = \frac{4\pi G M^2}{\hbar c \ln 2} \propto M^2 \tag{2}$$

i.e. at a given scale a black hole carries the largest amount of information. The amount of information grows as the square of the mass M.

2.2 The Earth, the Sun and neutron stars

The recurrence of the domain–boundary spatial organization established in our earlier report [1] is also found among macroscopic and even extreme celestial objects. If we set aside for the moment the complex dynamical mechanisms of the various disciplines and compare intuitively only spatial geometric structure and the known layering, the Earth, the Sun and neutron stars, three entirely different objects, likewise show similar nested domain–boundary features, as shown in Fig. 2.

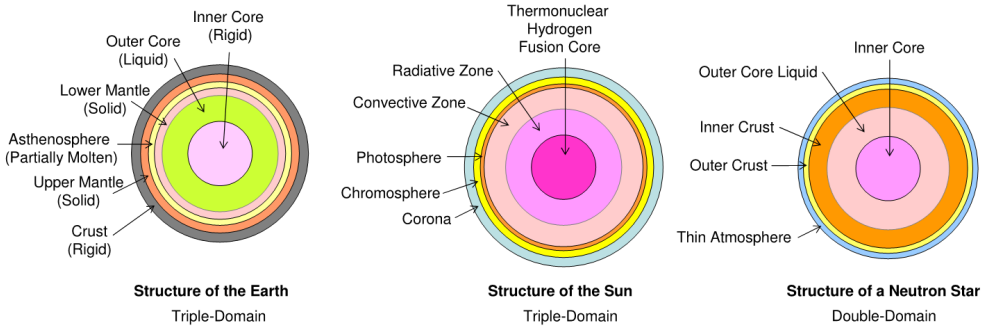

Fig. 2 Schematic structure of the earth, the sun and a neutron star

Terrestrial planets (the Earth as an example). In spatial structure, the Earth shows a clear division into layers from the inside out. At the centre is the solid inner core, surrounded by a very thick, hot liquid outer core. Between the deeper solid mantle and the rigid lithosphere (the crust together with the uppermost mantle), i.e. within the upper mantle, lies the asthenosphere, whose material is hot, highly viscous and able to flow slowly, and which acts structurally as a transition and buffer. The outermost layer is the familiar solid crust, which forms the classical physical boundary between the planet and space. The asthenosphere beneath the lithosphere is the underlying reason why continental plates can move. From the centre to the surface the layers alternate as solid → liquid → solid → semi-fluid → solid, a clear three-domain–three-boundary structure.

Stars (the Sun as an example). At the very centre is the core, where nuclear fusion takes place; it is enveloped in turn by the radiative zone and the convective zone,

where energy is carried outward slowly through countless scatterings and convection, forming a large intermediate buffer phase; the energy is finally radiated into space through the photosphere and chromosphere. The energy carrier undergoes the reversal "radiative zone (mainly photons) → convective zone (mainly plasma) → photosphere (mainly photons)", and the three-domain–three-boundary structure is expressed in this reversal of the energy carrier.

Neutron stars. A neutron star is the compact remnant left after gravitational collapse and a supernova at the end of stellar evolution, with a mass of about 1.35–2.1 solar masses and a radius of only about 10–14 km (diameter about 20–28 km), supported against gravity by neutron degeneracy pressure; above the TOV limit (about 2.2–2.3 solar masses) it collapses into a black hole (Section 3.2 gives the criterion for this collapse in the present framework). From the inside out there are the inner core (superfluid neutrons and superconducting protons), the liquid outer core, the inner crust (a mixture of solid lattice and superfluid), the outer crust (a lattice of heavy nuclei and free electrons) and an extremely thin atmosphere, the layers evolving as semi-fluid → fluid → semi-fluid → solid. Because a neutron star comes from a burnt-out star, the original three-domain–three-boundary structure degenerates into a two-domain–two-boundary structure.

2.3 Interface structure of black holes and the mapping to eukaryotic cells

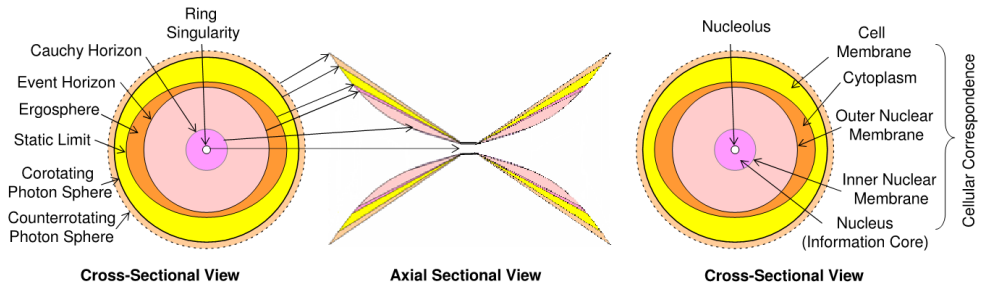

Fig. 3 Schematic structure and cellular correspondence of a Kerr black hole

Under extreme gravitational conditions, a rotating Kerr black hole is also depicted in its spatial structure as a regular nested domain–boundary hierarchy, as shown on the left of Fig. 3. At the very centre is the ring singularity, isolated by the inner Cauchy horizon; in the middle is a region called the ergosphere, where, because of strong frame dragging, any matter entering is forced to co-rotate; it forms a special intermediate transition zone between the event horizon on the inside and the static limit on the outside; finally, the whole system connects on the outside through the photon sphere (for a Kerr black hole, strictly a photon region) to the asymptotically flat classical space of the universe.

This structure corresponds systematically to a eukaryotic cell in geometry and function (right of Fig. 3): the photon sphere corresponds to the cell membrane, the ergosphere to the cytoplasm, the event horizon to the outer nuclear membrane, the Cauchy horizon to the inner nuclear membrane, the interior to the nucleus, and the ring singularity to the nucleolus. The black hole is the basic "cell" unit of the universe; its unified organizational information divides into a bulk part and a surface part (Eq. (1)): the outer horizon registers its surface information Ψ_s and the inner horizon its bulk information Ψ_b (see Section 2.4):

$$\Psi(BH) = \Psi_b(BH) + \Psi_s(BH) \tag{3}$$

The position of the inner nuclear membrane. Paper II [2] obtained the inner-interface radius ℓ_p of a single capsule from the force balance of the spacetime interfacial tension. Generalizing to a black hole of energy E: let the energy E be distributed uniformly as a massless field in a sphere of radius R, with $p = \rho/3 = E/(4\pi R^3)$; cutting along the equatorial plane, the force pushing the two halves apart is $F_{push} = p \cdot \pi R^2 = E/(4R)$; the spacetime interfacial tension $\tau = c^4/(8\pi G)$ gives a pull of $\pi\tau$ at each of the inner and outer interfaces, $F_{pull} = 2\pi\tau = c^4/(4G)$ in all, independent of the radius [2]. Equating the two gives the inner-interface radius of the black hole,

$$R_i = \frac{GE}{c^4} = \frac{R_s}{2} \tag{4}$$

In terms of the capsule number, $R_i = N\ell_p$ and the outer interface is $R_o = R_s = 2N\ell_p$ (the horizon radius of a Schwarzschild black hole of the same mass), the ratio of the two being always 1:2. R_i depends only on the total energy, not on the spin, and is the boundary that confines the E_c capsule packs: in both Schwarzschild and Kerr black holes the capsule packs lie within R_i; R_i itself stores no separate information, the information being registered on the horizons. A Schwarzschild black hole has no inner horizon, and the inner nuclear membrane corresponds to the inner interface R_i; the inner nuclear membrane of a Kerr black hole is the Cauchy horizon (Section 2.4). The inner interface is a structure of the cell model of this paper.

What the nucleus contains. According to Paper III, the interior of a black hole consists of N capsules E_c, and the entropy $S/k_B = 4\pi N^2$ is exactly the sum of the self terms of all capsules and their ordered pairwise relations, with no many-body terms; each pack is registered with the sequence number at which it entered, and the sequence number fixes its packing temperature $k_B T_N^+ = E_P/[4\pi(2N+1)]$ and characteristic wavelength; unpacking follows the last-in-first-out rule [3]. The "organizational code" of a black hole is this set of relations registered in order: it records the whole history of the black hole, which is the counterpart of the cell nucleus as the repository of genetic information. Paper II [2] pointed out that the capsule energy density ρ_c is the upper limit of actual physical density, so there is no singular point of infinite density inside a black hole; in the present framework the ring singularity in Fig. 3 corresponds to the position of the innermost nucleolar structure in the nucleus.

From the outside in, a black hole therefore shows a gradient from manifest to hidden: outside the horizon are unpacked matter and radiation (explicate order), inside

the horizon are the packed E_c and their relations (implicate order); the conversion between the two is packing and unpacking, taking place at the inner interface R_i, with the relations registered on the horizons [3].

2.4 Inner and outer horizons of a Kerr black hole and the distribution of information

Paper III extended the entropy counting to Kerr black holes [3]; this section quotes its results and only assigns the domain–boundary distribution of information to the two horizons. A Kerr black hole of mass M and angular momentum J has two horizons $r_\pm = GM/c^2 \pm \sqrt{(GM/c^2)^2 - a^2}$, with $a = J/(Mc)$, $r_+ + r_- = R_s$ and $r_+ r_- = a^2$; $r_\pm$ are coordinate values, the size of a horizon is given by its area, and the radius defined by area is $R_{A\pm} = \sqrt{A_\pm/4\pi} = \sqrt{R_s r_\pm}$. According to Paper III, the entropies of the two horizons are each obtained independently from their own areas [3]:

$$S_+ = 4\pi k_B N_{irr}^2, \qquad S_- = 4\pi k_B \left(N^2 - N_{irr}^2\right), \qquad S_+ + S_- = 4\pi k_B N^2 \tag{5}$$

where $N = M/m_P$ counts the total mass and $N_{irr} = M_{irr}/m_P$ the irreducible mass. Geometrically, the sum of the two horizon areas is [3]

$$A_+ + A_- = 4\pi R_s \left(r_+ + r_-\right) = 4\pi R_s^2 \tag{6}$$

i.e. the sum of the two horizon areas equals exactly the horizon area of a Schwarzschild black hole of the same mass. This relation has three layers of meaning. First, the total is fixed by the mass alone: $R_s = 2GM/c^2$ is independent of the spin and corresponds to the total number of relations N^2 of Paper III (entropy $4\pi k_B N^2$). Second, the spin fixes only the distribution: the equatorial circumference of both horizons is always $2\pi\sqrt{g_{\phi\phi}}\,|_{\theta=\pi/2} = 2\pi(r_\pm^2 + a^2)/r_\pm = 2\pi R_s$, independent of the spin; rotation makes the horizon contract along the meridians without stretching the equator, and the area that the outer horizon loses relative to a Schwarzschild black hole of the same mass, $4\pi R_s^2 - A_+ = 4\pi R_s(R_s - r_+) = 4\pi R_s r_- = A_-$, is transferred exactly to the inner horizon. Without rotation all the area is on the outer horizon ($A_- = 0$); the faster the rotation, the more area is transferred to the inner horizon. Third, this provides the geometric carrier of the unified organizational information $\Psi = \Psi_b + \Psi_s$ (Eq. (1)): the outer horizon registers the surface information, the inner horizon the bulk information, and their sum is locked by the mass. Note that Eq. (6) holds at given mass; when a black hole accretes or merges its mass changes and the total changes with it, which is the process of pack-by-pack registration and growth of the total number of relations described in Paper III [3]. Inside a black hole there are only the rest-massless E_c packs registered in order and no other structures that can carry information, so the storage of information falls on the horizons: when the bulk loses its structure, the storage of information moves to the surface (Section 2.1), and information that belonged to the bulk becomes surface information registered on the outer horizon. A Schwarzschild black hole has no inner horizon, $\Psi_b = 0$ and $S_- = 0$: it has no surface on which bulk information is registered, and what is registered on its outer horizon is all of its

information; the rotation of a Kerr black hole is an internal degree of freedom, and the bulk information it brings is registered on the inner horizon.

Accordingly, the decomposition of unified organizational information (Eq. (3)) corresponds term by term to the entropies of the two horizons of a Kerr black hole: the outer-horizon entropy S_+ corresponds to the surface information Ψ_s and the inner-horizon entropy S_- to the bulk information Ψ_b:

$$\Psi(BH) = \Psi_s(BH) + \Psi_b(BH) \;\leftrightarrow\; S = S_+ + S_- = 4\pi k_B N^2 \tag{7}$$

The inner interface and the two horizons. From $r_+ + r_- = R_s$, $R_i = R_s/2 = (r_+ + r_-)/2$ is exactly the midpoint of the two horizons in the coordinate sense; from Eq. (6), $R_{A+}^2 + R_{A-}^2 = R_s^2$, so $R_i = \frac{1}{2}\sqrt{R_{A+}^2 + R_{A-}^2}$, and the sum of the two horizon areas is always four times the area of the inner interface, $A_+ + A_- = 4A_i$, $A_i = 4\pi R_i^2$.

2.5 Mapping to biological cells: the prokaryote/eukaryote division

According to Paper III [3], $R_{A+} = R_s \cos\omega$, $R_{A-} = R_s \sin\omega$ and $\chi = \sin 2\omega$, where 2ω is the spin angle. At low spin $R_{A-} < R_i$; at high spin $R_{A-} > R_i$. The crossing point is at $R_{A-} = R_s \sin\omega = R_i = R_s/2$, which gives $\omega = \pi/6$ and $\chi = \sin 2\omega = \sqrt{3}/2$. For $\chi < \sqrt{3}/2$ the inner horizon lies within R_i, and R_{A+} corresponds to a single cell membrane (prokaryotic type); for $\chi > \sqrt{3}/2$ both horizons (R_{A+}, R_{A-}) lie outside R_i, corresponding to a double membrane (eukaryotic type: outer nuclear membrane, inner nuclear membrane and perinuclear space), while all capsule packs still lie within R_i.

The division point $\chi = \sin 2\omega = \sqrt{3}/2$ has an independent basis: it coincides with the critical value given by Smarr for embedding the outer horizon [22]; for $\chi > \sqrt{3}/2$ the Gaussian curvature at the poles of the outer horizon becomes negative. Observationally, the spins of black-hole merger products are mostly around 0.7 [23], of prokaryotic type; among supermassive black holes grown by accretion, many have spins above 0.9 [24], of eukaryotic type. The egg cell is a eukaryotic cell, so a cosmic egg cell must be eukaryotic, $\chi > \sqrt{3}/2$; accretion that brings in enough net angular momentum can make a black hole evolve from the prokaryotic to the eukaryotic type; at the division $\sin\omega = 1/2$ and $\cos\omega = \sqrt{3}/2$, whereas $\cos\omega = N_{irr}/N$ is rational and $\sqrt{3}/2$ is irrational, so no integer state lies exactly on the division, but adjacent allowed states can cross it in one step (Paper IV [4], Section 3.1); the burst criterion [3, 4] lies at $\omega_{\max}$, deep in the eukaryotic region, with $\chi_{\max} = \sin 2\omega_{\max} = 1 - 1/N^2$; for large N, $\omega_{\max} \to \pi/4$.

Two points require comment. (1) In classical general relativity, the infinite blueshift of infalling radiation near the Cauchy horizon causes mass inflation [25], and the Cauchy horizon was therefore once regarded as unstable; more recent rigorous results show that the metric can be continuously (C^0) extended across the Cauchy horizon, although the curvature is generically expected to diverge [26]. In the present framework [3], packing takes place only at the inner interface R_i and the inner horizon

only registers relations; for $\chi < \sqrt{3}/2$ the inner horizon lies within R_i, in the capsule region, where the capsule environment is transparent inwards and there is no cross-flow of energy of the kind needed for mass inflation; for $\chi > \sqrt{3}/2$ the blueshift is cut off by the ring criterion before the local energy reaches E_P, and the one-way re-registration of rotational packs as irreducible packs further suppresses fluctuations near the inner horizon. (2) The existence criterion for black holes [3]: the two horizons are independent spacetime-geometric interfaces, and the difference of their areal radii is not smaller than $2\ell_p$, i.e. $R_{A+} - R_{A-} = R_s\sqrt{1-\chi} \geq 2\ell_p$; a separation equal to $2\ell_p$ is the existence boundary, and below it the structure breaks: the information registered on the two horizons mixes and can no longer be distinguished, leading to structural breakdown; the classical extremal point at which the two horizons coincide cannot be reached (Paper IV [4], Section 6). The allowed states are the integer range $\left\lceil \frac{1+\sqrt{2N^2-1}}{2} \right\rceil \leq N_{irr} \leq N$ (Paper IV [4], Section 3.2), and black holes with $N \leq 4$ do not rotate. This criterion is the basis of black-hole bursts (Section 4.3).

3 E_c capsules and black holes: two levels of basic units

We regard the matter–spacetime organization of the universe as built from two levels of basic units: the capsule E_c is the basic unit of the background energy–spacetime, and the black hole is the basic unit of the foreground matter skeleton. Their relation resembles that between proteins and cells: proteins are among the molecular building blocks of cells, and cells are functional units organized from molecular units and capable of independent activity.

3.1 The capsule E_c

The geometry, energy and boundary constraints of the capsule E_c were given in Paper II [2]: inner diameter $2\ell_p$, outer diameter $4\ell_p$, volume $V_c = (32\pi/3)\ell_p^3$, energy E_P, with the outer interface lying exactly at the Schwarzschild radius of E_P. Paper III further showed [3] that a pack of E_P is self-bound and that a single E_c can neither pack nor unpack; the E_c of the cosmic background are therefore stable and do not decay into radiation, and there is no radiation from E_c in cosmic voids. This is necessary for E_c to be the unit of dark energy. The capsule creation-rate equation of Paper II describes the replenishment of background capsules as the universe expands, keeping the capsule density constant; it is a process different from packing by black-hole accretion and from unpacking at a burst.

Hence E_c exists in two states: free in the cosmic background, or as capsule packs inside black holes. The former are the units of dark energy, the latter the units of dark matter. E_c does not destroy itself to "materialize"; it "materializes" as radiation only when a black hole unpacks (Section 5.4).

3.2 The unified density criterion for black-hole formation

A Schwarzschild black hole containing the energy of N capsules has mass $M = Nm_P$ and horizon radius $R_s = 2N\ell_p$ [2]; its mean density is

$$\bar{\rho}(N) = \frac{Nm_P}{\frac{4}{3}\pi\,(2N\ell_p)^3} = \frac{Nm_P}{\frac{32\pi}{3}N^3\ell_p^3} = \frac{m_P}{\frac{32\pi}{3}\ell_p^3}\cdot\frac{1}{N^2} = \frac{\rho_c}{N^2} \tag{8}$$

where $\rho_c = m_P/V_c$ is the mean density of a single capsule:

$$\rho_c = \frac{2.176\times10^{-8}\ \text{kg}}{\frac{32\pi}{3}\times(1.616\times10^{-35}\ \text{m})^3} \approx 1.54\times10^{95}\ \text{kg/m}^3 \tag{9}$$

This gives the formation criterion for black holes: **a region whose energy is NE_P and whose density reaches ρ_c/N^2 forms a black hole of N capsules.** This is equivalent to the condition of general relativity that "a mass M is compressed within its own Schwarzschild radius", expressed in terms of the capsule number; its significance is that it unifies the formation of black holes on all scales under a single criterion.

The smallest black hole. For $N = 2$, $\bar{\rho} = \rho_c/4$: one capsule enters as a whole the inner cavity of the other capsule as unfolded, inscribed in the inner interface of radius $R_i = 2\ell_p$, the horizon radius being $R_s = 4\ell_p$; it is an unstable transitional state between packing and unpacking, evaporates immediately after forming, and is of significance only in principle.

Large N: stellar collapse. A neutron star whose mass exceeds the TOV limit (about 2.2–2.3 $M_\odot$) collapses into a black hole. The capsule number at this mass, and the mean density required by the formation criterion, are

$$\begin{aligned} N &= \frac{M}{m_P} = \frac{(2.2\text{–}2.3)\times1.989\times10^{30}\ \text{kg}}{2.176\times10^{-8}\ \text{kg}} \approx (2.0\text{–}2.1)\times10^{38}, \\ \bar{\rho} &= \frac{\rho_c}{N^2} = \frac{1.54\times10^{95}\ \text{kg/m}^3}{(2.0\text{–}2.1)^2\times10^{76}} \approx (3.5\text{–}3.8)\times10^{18}\ \text{kg/m}^3 \end{aligned} \tag{10}$$

This mean density is comparable to the central density of neutron stars (of order 10^{18} kg/m^3), so the criterion agrees with the existing theory of neutron-star collapse. Stellar-collapse black holes therefore need no pre-existing black-hole core: once the collapsing core satisfies Eq. (8), a black hole of $N \sim 10^{38}$ capsules forms directly. Primordial and stellar-collapse black holes differ only in where, and with what N, the criterion is satisfied, not in being two different formation mechanisms.

3.3 Formation and survival of black holes in the early universe

The density clock. Matter in the parent universe starts from the density ρ_c of the capsule packs themselves and passes through all lower densities as the universe expands. To compare with the timeline of standard cosmology, we use a "density clock" to express the local density. In a radiation-dominated flat universe the Hubble

parameter H (the expansion rate of the universe; its present value is H_0) is $H = 1/(2t)$, and the density is related to time t by

$$\rho(t) = \frac{3H^2}{8\pi G} = \frac{3}{32\pi G t^2} \tag{11}$$

Conversely, the time $t \equiv \sqrt{3/(32\pi G\rho)}$ corresponding to a local density ρ is the reading of the density clock for matter there. It is a local quantity, unrelated to the Hubble sphere; the Hubble sphere belongs only to the universe as a whole (Section 4.2).

Setting $\rho(t) = \rho_c/N^2$ and substituting $\rho_c = m_P/[(32\pi/3)\ell_p^3]$:

$$N^2 = \frac{\rho_c}{\rho(t)} = \frac{m_P}{\frac{32\pi}{3}\ell_p^3} \cdot \frac{32\pi G t^2}{3} = \frac{G m_P\, t^2}{\ell_p^3} \tag{12}$$

From $\ell_p = G m_P/c^2$ we have $G m_P = \ell_p c^2$, so $N^2 = c^2 t^2/\ell_p^2$, i.e.

$$N = \frac{t}{t_P}, \qquad M = N m_P = \frac{m_P}{t_P}\, t = \frac{c^3 t}{G} \tag{13}$$

where $t_P = \ell_p/c$, and the last step uses $m_P/t_P = m_P c/\ell_p = c^3/G$. Equation (13) is a criterion on the local density: a black hole formed directly where the density clock reads t contains $N = t/t_P$ capsules. The density clock starts from the density of the capsule itself, ρ_c ($t = t_P$). $M = c^3 t/G$ has the same form as the horizon-mass estimate in the primordial-black-hole literature [27], but here it comes only from the local criterion ρ_c/N^2. Whether a region satisfying the criterion collapses into a black hole or continues to dilute with the expansion is decided, in the standard picture of random fluctuations, by the threshold δ_{th} of the density contrast $\delta = \delta\rho/\rho$; the classic estimate is $\delta_{th} \approx 1/3$ [28], and more recent analytic and numerical results give about 0.4–0.6 (depending on the amplitude definition used) [29]; we hold that where collapse occurs is decided by the organizational code as the new universe unfolds, not by purely random fluctuations.

Critical mass and evaporation. Whether a black hole can grow depends on its temperature relative to the background: when the Hawking temperature is below the background temperature it absorbs on balance, and when above it evaporates on balance [3]. Setting the Hawking temperature equal to the background temperature gives the critical mass

$$M_{crit}(t) = \frac{\hbar c^3}{8\pi G k_B T_{bg}(t)} \tag{14}$$

The background temperature follows from the radiation energy density $\rho(t)c^2 = (\pi^2/30)\, g_* \big(k_B T_{bg}(t)\big)^4/(\hbar c)^3$ together with Eq. (11):

$$k_B T_{bg}(t) = \left(\frac{45\,\hbar^3 c^5}{16\pi^3 g_*\, G\, t^2} \right)^{1/4} \tag{15}$$

where g_* is the effective number of relativistic degrees of freedom, which changes stepwise with temperature. Since $T_{bg} \propto t^{-1/2}$, $M_{crit} \propto t^{1/2}$; the red line in Fig. 4 is $M_{crit}(t)$. The concept of a critical mass has been proposed before: Custódio and Horvath equated the rates of radiation absorption and Hawking evaporation and obtained $m_c \propto T^{-1}$ [30]. By detailed balance, emission and absorption between a black hole and a radiation bath at the same temperature are exactly equal, so rate balance and temperature balance are the same condition. We use temperature balance, whose physical picture is more direct.

Figure 4 integrates the net rate of absorption and emission of the black-hole mass step by step:

$$\frac{dM}{dt} = \frac{\pi^2 \sigma}{30\,\hbar^3 c^4} \left[g_* \big(k_B T_{bg}\big)^4 - g_* \big(k_B T_H\big)^4 \right] \tag{16}$$

The first term in the brackets is the background radiation absorbed by the black hole and the second the radiation it emits at its own temperature; both have the Stefan–Boltzmann form of blackbody radiation, with g_* taken at the respective temperature. The background temperature T_{bg} is given by Eq. (15) and decreases with time; the black-hole temperature, $k_B T_H = \hbar c^3/(8\pi G M)$, decreases with mass. When the two temperatures are equal, $dM/dt = 0$, which is the critical mass of Eq. (14); for $T_{bg} > T_H$ the black hole absorbs on balance and for $T_{bg} < T_H$ it evaporates on balance. σ is the absorption cross-section; absorption and emission use the same cross-section, which cancels in the equilibrium condition and affects only how fast the black hole grows or evaporates.

Equation (16) treats the black hole as a blackbody: all radiation falling on the cross-section is absorbed, and emission is computed with the same cross-section. Outside a real black hole the curved spacetime acts as a barrier, and low-energy quanta with wavelengths comparable to R_s are partly reflected, so both absorption and emission are smaller than for a blackbody and depend on the particle species; this is called a greybody. Computing the greybody effect species by species for all Standard Model particles ($g_* = 106.75$) gives the grey-body-corrected evaporation lifetime [31]

$$t_{ev,\mathrm{grey}} \approx 6.25 \times 10^{-18}\, \frac{M_0^3}{f} = 77.8\, N^3 t_P \tag{17}$$

where $M_0 = N m_P$ is the initial mass of the black hole and $f = 15.35$ is the weight when all Standard Model particles are counted.

Let s denote the ratio of the effective absorption cross-section of the black hole to the geometric-optics cross-section, so that $\sigma = s \cdot 27\pi G^2 M^2/c^4$. Substituting into Eq. (16), keeping only the emission term and taking g_* as the constant 106.75, integration gives the evaporation lifetime of the blackbody model

$$t_{ev,\mathrm{black}} = \frac{40960\pi G^2 M_0^3}{27 s g_* \hbar c^4} = \frac{40960\pi}{27 s g_*}\, N^3 t_P \tag{18}$$

Setting $t_{ev,\mathrm{black}} = t_{ev,\mathrm{grey}}$ gives

$$s = \frac{40960\pi}{27 \times 106.75 \times 77.8} = \frac{1.287 \times 10^5}{2.242 \times 10^5} = 0.574 \tag{19}$$

that is, under the above calibration of particle degrees of freedom and lifetime, the mean effective grey-body correction factor is about 0.574, i.e. the effective absorption cross-section is on average about 57% of the geometric-optics cross-section.

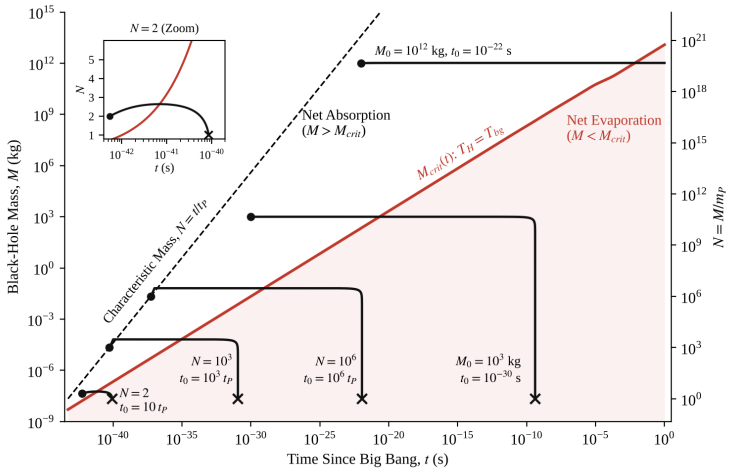

Fig. 4 Early-universe black holes relative to the critical mass $M_{crit}(t)$ (red; $T_H = T_{bg}$). Dashed: characteristic formation mass $N = t/t_P$. Each black curve is labelled with its initial mass and formation time (inset: $N = 2$; $N = 2$ forms by capsule contact and lies below the characteristic line); dots mark formation and crosses complete evaporation; the $M_0 = 10^{12}$ kg black hole survives. Right axis: $N = M/m_P$

Figure 4 shows several kinds of trajectories of early black holes relative to the critical mass. The red line is $M_{crit}(t)$, the mass at which the Hawking temperature equals the background temperature: above the red line a black hole absorbs on balance and its mass increases with time; below it, it evaporates on balance and its mass decreases. The black dashed line is the characteristic mass $N = t/t_P$ formed according to Eq. (13); it increases with time and always lies above M_{crit}: at $t = 10^{-40}$ s, $M = 4.0 \times 10^{-5}$ kg while $M_{crit} = 2.2 \times 10^{-7}$ kg; at $t = 10^{-20}$ s, $M = 4.0 \times 10^{15}$ kg and $M_{crit} = 2.2 \times 10^{3}$ kg. (1) The smallest, $N = 2$ black hole (see the inset), formed at $10\,t_P$, grows briefly, is overtaken by $M_{crit}(t)$ and evaporates within about 10^{-40} s. An $N = 2$ black hole forms by the contact of two capsules, whose local density is $\rho_c/4$, and does not require the local mean density to satisfy Eq. (13); it therefore lies below the characteristic line (the mean density at $10\,t_P$ is $\rho_c/100$). It forms only during the rapid-creation stage, in which capsules are in mutual contact, and its fate after formation is still decided by $M_{crit}(t)$. (2) Black holes formed at the characteristic mass ($N = 10^3$ formed at $10^3\,t_P$; $N = 10^6$ formed at $10^6\,t_P$) are all in the net-absorption

region when they form, but the growth from absorption is limited, at most a few times (3 times in the figure) [27, 32]; thereafter $M_{crit}(t)$ catches up with them, they turn to net evaporation, and they evaporate completely at about 1×10^{-31} s and 1×10^{-22} s respectively. (3) Heavier ones, such as 10^3 kg (formed at 10^{-30} s), evaporate at about 4×10^{-10} s; 10^{12} kg (formed at 10^{-22} s) survives to the present. The mass-loss rate due to evaporation, $|dM/dt|$, is proportional to M^{-2}, and a black hole loses most of its mass in the last stage of its life, so the fall is nearly vertical on a logarithmic time axis. Survival to the present is decided by the evaporation time, which is proportional to M^3; a lifetime longer than the age of the universe requires $M \gtrsim 5 \times 10^{11}$ kg [31], so the survival condition is a mass condition. By Eq. (8), the capsule number and the local density required to form such a black hole directly are

$$\begin{aligned} N &= \frac{M}{m_P} = \frac{5 \times 10^{11}\ \text{kg}}{2.176 \times 10^{-8}\ \text{kg}} \approx 2.3 \times 10^{19}, \\ \rho &= \frac{\rho_c}{N^2} = \frac{1.54 \times 10^{95}}{(2.3 \times 10^{19})^2}\ \text{kg/m}^3 \approx 2.9 \times 10^{56}\ \text{kg/m}^3 \end{aligned} \tag{20}$$

Black holes formed directly where the local density is higher than this value all have masses below 5×10^{11} kg and will eventually evaporate; only larger black holes formed where the density is lower can survive and keep growing. The starting point of black holes is therefore still $1 + 1 = 2$, but the earliest ones all disappear quickly.

The smallest, $N = 2$ black hole in Fig. 4 represents one round of the $1+1 \to 2 \to 1$ cycle in the early stage of the burst: two neighbouring E_c combine into an $N = 2$ black hole, and evaporation ends with $2 \to 1$, emitting one pack E_P of radiation and leaving one E_c [3]. The intrinsic density of background capsules is always ρ_c, and the capsules created rapidly in the early stage of the burst are in contact as soon as they appear, so as long as creation continues, such cycles recur everywhere; how long they last is set not by the mean density but by the duration of the creation stage. The radiation of the early hot state accumulates from this cycle.

This picture is isomorphic to crystallization from solution. In a solution, nuclei smaller than the critical size redissolve and only those larger than it can grow; the smaller the particle, the more soluble it is (the Gibbs–Thomson effect) [33]. The smaller a black hole, the hotter it is and the more easily it evaporates, and $M_{crit}(t)$ is exactly the "critical nucleus" line. The heat capacity of a black hole is negative, so the larger absorb and the smaller evaporate, just as in Ostwald ripening large crystals grow and small ones dissolve [33].

3.4 Growth of black holes: accretion packing and mergers

Black holes grow in two ways, both given in Paper III [3]. In accretion, the outer horizon accepts only unpacked energy, which accumulates share by share in sub-step energy shares $\varepsilon_N = E_P/(2N + 1)$ matched to the Hawking temperature at the time; when a full E_P has been gathered at the inner interface R_i it forms a pack, and each pack is registered on the horizon with the sequence number at which it entered; E_c already packed in the cosmic background are not drawn in by the outer horizon; energy changes in whole packs of E_P and area in sub-steps of A_o. When accretion brings in

angular momentum, the upper limit of the spin is constrained by the existence criterion for black holes (Section 2.5). In a merger, a common outer interface forms outside the two horizons; the smaller black hole dissolves while its capsules do not, being absorbed as a whole and attached in their original order after those of the larger black hole; the group relations between the two before the merger are converted into $2N_1N_2$ cross relations, and the $N_u < N_2$ packs that leave the irreducible part are unpacked from the tail of the sequence and carried away by gravitational waves and rotational energy, so that information is conserved across the merger. In GW150914 about 25% of the capsules of the secondary black hole leave the irreducible part, whereas GW190814, with its very unequal mass ratio, is closer to absorption as a whole [3].

No sub-black holes are retained after a merger: if the progenitors were retained as complete units, the entropy would exceed the value uniquely fixed by the area [3]. This is the counting form of the no-hair theorem, and corresponds in biology to the reorganization of previously independent units into a higher-level integrated organization.

3.5 Black-hole cores inside celestial bodies

Section 2.2 regarded the Earth, the Sun and neutron stars as nested domain–boundary structures; a natural question is whether a celestial body could have a black-hole core at its centre. Our view is as follows.

For a primordial black hole to dominate the condensation of the surrounding gas and become the nucleus of a star, its mass would have to approach the Jeans mass of the surrounding gas, i.e. the order of a solar mass; a black hole that large gathering gas forms an accreting black hole, not an ordinary star. A low-mass primordial black hole has a tiny gravitational reach; it can affect the local evolution of nearby gas but can hardly dominate the overall condensation, and is mostly engulfed passively by a star as it forms. The probability of engulfment depends on the environment: the higher the dark-matter density and the slower its motion, the easier the engulfment.

Population III stars (the earliest stars in the universe, almost free of heavy elements and not yet directly observed) formed in minihaloes of high dark-matter density and low velocity dispersion. In the present framework (dark matter consists of black holes), these stars are likely to have engulfed surrounding primordial black holes as they formed; Bambi et al. pointed out that several black holes engulfed by a star can sink to the centre of the star by dynamical friction and merge into a single black hole, thereby affecting the lifetime and fate of the star [34]. Present-day ordinary stars form in galactic discs, where dark matter moves fast, and the probability that a star engulfs a black hole as it forms is very low. Bellinger et al. studied the Sun with a central black hole using complete stellar-evolution models and found that black holes below about $10^{-6}\,M_\odot$ would not change the present structure of the Sun significantly, but that, judging from existing observations, the Sun very probably has no black hole at its centre [35]. For the capture of primordial black holes in stars and compact stars and the corresponding constraints, see Refs. [36–39]. Hence, if dark matter consists of black holes, Population III stars are rather likely to contain black-hole cores, how commonly depending on the capture probability and on the mass spectrum of primordial black holes, while present-day ordinary stars are very unlikely

to contain one. If an individual star does contain a black-hole core, the lower limit of its mass is set by the survival condition (5×10^{11} kg) [31] and the upper limit by stellar structure. These conclusions depend on the premise that "dark matter consists of black holes", which is still disputed.

3.6 Mass spectrum, clustering and detection

Mass spectrum. By Eq. (8), the formation mass of primordial black holes varies with the local density where they form, effectively continuously at large N, and the masses of surviving primordial black holes start from 5×10^{11} kg. Thereafter black holes keep growing by accretion and mergers, and stellar collapse gives black holes of several solar masses according to Eq. (10), so the overall mass spectrum of black holes is extended. Narrow-spectrum models in the literature (approximately δ-function) arising from local features of the inflaton potential [40] agree with the picture of this paper: primordial black holes formed mainly during a certain period after the burst of the parent black hole, with masses concentrated in a narrow spectrum; black holes can also form outside the narrow mass range, but with small probability, forming only a sparse tail of the spectrum. The mass spectrum of primordial black holes is therefore "a narrow peak plus a sparse long tail", which together with stellar-collapse black holes makes up the extended overall mass spectrum.

The asteroid-mass window. Primordial black holes of mass 10^{14}–10^{19} kg are not yet excluded by observation [41, 42]. They contain $N = M/m_P \approx 4.6 \times 10^{21}$–$4.6 \times 10^{26}$ capsules, formed where the local density was $\bar{\rho}(N) = \rho_c/N^2 \approx 7 \times 10^{51}$–$7 \times 10^{41}$ kg/m^3, and their lifetimes far exceed the age of the universe: the evaporation time is proportional to M^3; a black hole of 5×10^{11} kg has a lifetime about equal to the age of the universe, and one of 10^{14} kg already about 10^7 times longer.

Clustering. Primordial black holes may be highly clustered, driven by nonlinear density fluctuations in the early universe [16, 43], forming black-hole clusters with local densities far above the mean. Clustering makes lensing paths along the line of sight overlap, which may cause microlensing surveys to miss them systematically [14], and also makes binary black-hole mergers more frequent [15].

An analysis of the underlying limitation of microlensing and dark-matter detection. Over more than 30 years of microlensing surveys (since the preparation of EROS/MACHO in 1989), astronomy has relied throughout on visible/near-infrared wavelengths (400–800 nm, silicon CCD detectors). As a result, none of the microlensing data accumulated over these 30-odd years can, as a matter of basic physics, cover primordial black holes in the asteroid-mass window (horizon radii 0.00015–15 nm, masses 10^{14}–10^{19} kg). The measured detection limit of optical surveys is about 6.6×10^{18} kg [10]. When the wavelength of light exceeds the gravitational scale of the lens, wave optics replaces geometric optics; whether this regime is entered is decided by the wave parameter w_λ:

$$w_\lambda = \frac{4\pi R_s}{\lambda} \tag{21}$$

For $w_\lambda \gtrsim 1$ geometric optics holds and light is bent and magnified; for $w_\lambda \ll 1$ the geometric-optics approximation fails, the light wave passes around the black hole, and the magnification is suppressed by wave optics and tends to 1. For $\lambda = 500$ nm, black holes of 10^{14}–10^{19} kg have $w_\lambda \approx 4 \times 10^{-6}$–0.4, all in the wave-optics regime; this is the physical reason why optical surveys cannot cover the asteroid-mass window.

4 Cosmic egg cells, the parent black hole and black-hole bursts

4.1 The most massive black holes: cosmic egg cells

We regard the most massive black holes known in the universe, such as supermassive black holes of the TON 618 class (about $6.6 \times 10^{10} M_\odot$, $N \approx 6.0 \times 10^{48}$), as "cosmic egg cells": candidate nodes through which the present generation of the universe gives birth to the next. Naming convention: a black hole and a universe of the same generation are the states before and after the burst. The parent black hole burst into the parent universe, i.e. our universe. TON 618 lies in our parent universe and is itself called a child black hole; what it gestates is the child universe. A horizon is the carrier with the largest information capacity at a given mass [5, 8], so a black hole is the only form in which the organizational code of a universe can be stored completely and passed on to the next generation; that black holes become the link of cosmic inheritance is a necessary consequence of the law of information storage. By Section 2.5, a cosmic egg cell must be eukaryotic. One must distinguish the potential to become a cosmic egg cell from the actual development: just as many oocytes complete their pre-setting while only very few take part in reproduction, many primordial black holes may have reproductive potential, while only very few reach the breaking condition in later development.

4.2 Our universe lies within the parent Hubble sphere

Paper II [2] gave a known property of a flat universe: for the Hubble sphere of radius $R_\mathcal{H} = c/H$ containing mass $M_\mathcal{H}$,

$$M_\mathcal{H} = \frac{R_\mathcal{H} c^2}{2G}, \qquad R_\mathcal{H} = \frac{2GM_\mathcal{H}}{c^2} = R_S \tag{22}$$

It is only a scale defined by the expansion rate and has no physical binding power: it does not bind matter or stop light, matter and light can cross it in both directions, and the recession velocity on the Hubble sphere equals the speed of light. That it satisfies Eq. (22) means only that the Hubble sphere lies exactly at its own Schwarzschild radius; this is merely another way of writing the Friedmann equation of a flat universe and does not mean that the Hubble sphere is a black hole. The idea that the universe is the interior of a black hole is old [44, 45], and Smoller and Temple even regarded the Big Bang as a shock wave inside a black hole [46]; the difference here is that we count in E_c capsules, that after the burst the horizon converts into the Hubble sphere and retains the registered information, and that the dark-energy share accumulates

gradually with the creation of background capsules. The horizon of the parent black hole had binding power before the burst; after the burst it converted into the Hubble-sphere horizon and the binding was removed. In terms of capsules, $N_{\mathcal{H}} \approx 4.25 \times 10^{60}$ [2]; all the capsules were released and unfolded into the parent universe.

Each generation of universe has its own Hubble sphere. Taking our parent generation as an example: when the parent black hole burst, the registrations on its inner and outer horizons transferred together to the Hubble sphere of the parent universe (i.e. our universe): the sum of the two horizon areas, $A_+ + A_- = 4\pi R_s^2 = 16\pi N_b^2 \ell_p^2$ (Eq. (6)), converts into the area of the Hubble sphere. This is a conversion hypothesis proposed in this paper, the detailed process being left to future work. The initial radius and mean density of the Hubble sphere are

$$R_{\mathcal{H}0} = 2N_b \ell_p, \qquad \bar{\rho}_0 = \frac{\rho_c}{N_b^2} \tag{23}$$

where N_b is the number of capsules the parent black hole contained at the burst. Thereafter the Hubble sphere grows with the universe and always lies at its own Schwarzschild radius, which is why Eq. (22) holds at all times. The mean density $\bar{\rho}_0$ does not mean that the released E_c packs start from this low density: the ratio of the volume enclosed by the horizon to the volume occupied by the N_b capsule packs themselves is

$$\frac{\frac{4}{3}\pi \left(2N_b \ell_p\right)^3}{N_b V_c} = \frac{\frac{32\pi}{3} N_b^3 \ell_p^3}{N_b \cdot \frac{32\pi}{3} \ell_p^3} = N_b^2 \tag{24}$$

Each E_c pack has the constant density ρ_c, and the horizon volume is N_b^2 times the volume occupied by all the E_c packs; the mean density is the value spread over the whole horizon. The N_b packs released at the burst give the initial total amount of matter of the parent universe. If all the matter within today's Hubble sphere came from this single release, N_b would be of order $\Omega_m N_{\mathcal{H}} \approx 0.315 \times 4.25 \times 10^{60} \approx 1.3 \times 10^{60}$ (Ω_m being the matter density parameter), with mass $m_b = N_b m_P \approx 2.9 \times 10^{52}$ kg, about 2×10^{11} times that of TON 618.

We map the parent black hole only onto the Hubble sphere, counting N_b only out to $R_{\mathcal{H}}$; this is the account of one transfer, not a conservation relation. Most black holes in a universe stay in their own generation, and only very few reach the burst point. We make no inference about which generation the matter beyond the Hubble sphere comes from, and list the cross-generational energy balance as an open question.

Multi-level nesting of universes and the common E_c background. Outside black holes there is always the background E_c. This background may be shared by all generations of universes and has its own expansion rate. Hence the generations of universes coexist in a nested manner (Fig. 5): the horizon of each generation's black hole is, as seen from the previous generation's universe, a black hole, and after the burst it converts into the Hubble sphere of the universe of the same generation; black holes in the universe of the same generation in turn gestate the next generation. In Fig. 5, G1 is the ancestral universe and G2 the parent universe (i.e. our universe); both have burst, and their Hubble spheres are drawn dashed; G3 is a child black hole (such as TON 618), not yet burst, left–right symmetric, with its horizon drawn solid. All generations share the same E_c background, so any overlapping point has a

single temperature, and there are no multiple background temperatures belonging to different generations. The common background and the inherited organizational code may provide an organizing mechanism for establishing a uniform initial thermal state in widely separated regions that were never causally connected; whether this removes the horizon problem of standard cosmology requires further study. Observation gives constraints that this hypothesis must satisfy: COBE/FIRAS found the CMB to be a precise blackbody spectrum, $|y| < 1.5 \times 10^{-5}$ (the Compton y parameter, which measures the deviation of the spectrum from a blackbody) [47]; if radiation at different temperatures were superposed at the same point, the mixed spectrum would deviate from a blackbody; and the CMB temperatures T measured at different redshifts z all follow $T(z) = T_0(1 + z)$ [48]. Temperature and the background clock are therefore shared by all generations and cannot be used to distinguish them; the generations differ in matter and organizational code. If the overlapping region contains matter from an earlier generation, it may appear as objects older than the local age of the universe, which is a testable direction.

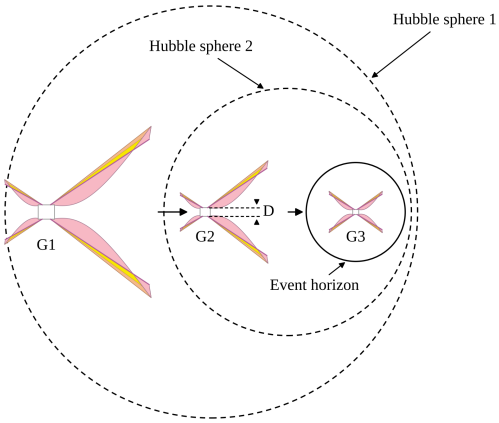

Fig. 5 Schematic of nested generations. G1: ancestral universe; G2: parent universe (our universe); G3: child black hole (e.g. TON 618), not yet burst. A black hole and the universe of the same generation are the states before and after its burst: at the burst the registrations on both horizons of the black hole transfer jointly to the initial Hubble sphere of that universe (dashed circles, Hubble spheres 1 and 2); the horizon of the unburst G3 is drawn solid. The Hubble spheres are defined by the expansion rate and exert no physical constraint; light from beyond them can reach the observer. The throat opening D of G2 is no smaller than one E_c diameter. All generations share the same E_c background, so any overlapping point has a single temperature

After the burst, the parent black hole does not break into fragments like a burst balloon, but persists for a considerable time as the remnant of the parent black hole. Our universe is the unfolding on the other side of its throat, which also gives a physical meaning to the statement that "the ancestral universe did not perish immediately after the burst of the parent black hole, but continues to evolve alongside the parent universe". Before the burst the black hole is at an extremely low temperature; after the burst the temperature of the remnant rises gradually towards the background

temperature but always stays below it, appearing in the CMB Cold Spot as the low-temperature shadow of the remnant (Section 6.2). After the burst the Hubble sphere grows with the parent universe. The Hubble sphere, however, is not a black hole, and the Hawking temperature cannot be computed from its mass–energy.

The inherited number of matter capsules N_b is fixed, while the capsule number within the Hubble sphere, $N_{\mathcal{H}}$, equals N_b only at the moment of the burst and thereafter changes with H, $N_{\mathcal{H}} = c/(2H\ell_p)$. The present relative rate of change of $N_{\mathcal{H}}$ is about 3.2% per billion years: small, without change of order of magnitude, but not negligible. $N_{\mathcal{H}}$ must be distinguished from two other counts. The Hubble sphere is not a fixed comoving volume, and the mass of matter in it also changes with time; the equivalent capsule number of the matter part is $N_m = \Omega_m N_{\mathcal{H}}$; at the burst $\Omega_m \approx 1$ and $N_m = N_{\mathcal{H}} = N_b$ (at the burst the inherited mass–energy consists entirely of capsule packs and the dark-energy residual is negligible relative to the total; "matter" here means the mass–energy of the inherited capsule packs, which differs in definition from Ω_m in the Planck data of Section 5.1); the actual number of background capsules in the Hubble sphere is of order $\phi N_{\mathcal{H}}^3$, contributing energy only through the residual, and it increases as the Hubble volume grows; this is the creation of background capsules with the expansion described in Paper II [2]. The three are different counts: N_b is the number of capsules inherited at the burst, $N_{\mathcal{H}}$ the equivalent capsule number of the total mass–energy of the Hubble sphere, and $\phi N_{\mathcal{H}}^3$ the actual number of background capsules.

The current cosmic timeline of standard cosmology: inflation (about 10^{-36}–10^{-32} s) [49–52] → reheating and particle production → electroweak phase transition (about 10^{-12}–10^{-6} s; elementary particles acquire rest mass through the Higgs mechanism) → Big Bang nucleosynthesis (about 10 s–20 min) → matter–radiation equality (about 50 000 years) → recombination and release of the CMB (about 380 000 years) → dark ages → reionization and Population III stars (about 100–500 million years). We are concerned with only two of these nodes: surviving primordial black holes begin to form once the local density falls below about 2.9×10^{56} kg/m^3 (Eq. (20)), far above the density of about 10^{20}–10^{33} kg/m^3 at the electroweak phase transition; and Population III stars form in minihaloes rich in primordial black holes.

4.3 Black-hole bursts: release as a whole, the throat jet, and recombination by code

A burst differs from evaporation. Paper III showed that for a whole pack of energy to cross the horizon as one quantum and evaporate into the space of the universe in which the black hole lies, the probability is suppressed to $\Gamma_{pack} = e^{-4\pi(2N-1)}$ [3, 53]. A black-hole burst is not such a process but an organizational phase transition of the whole, not constrained by the tunnelling probability.

A burst does not violate information conservation. Paper III forbids a black hole from "splitting in two", because the split would sever the $2N_1N_2$ relations between the two parts and reduce the entropy [3]. At a burst, the N packs, together with their N^2 registered relations carrying a total relational entropy of $4\pi k_B N^2$, pass as a whole into the new universe; the relations are not severed but converted from the registration order inside the black hole into the organizational code of the

new universe; the entropy does not decrease, and the second law is not violated. Evaporation and bursts are thus distinguished: evaporation severs relations pack by pack, and information flows out as radiation; a burst keeps the relations as a whole, making them the initial organization of the new universe.

The new universe unfolds on the other side of the black-hole throat: when the parent black hole bursts, the throat opens to one side, forming a local channel like the one-directional jet of a black hole. The diameter of the throat opening is no smaller than the diameter of one E_c, i.e. $D \geq D_o = 4\ell_p$. However large the opening, what passes through the throat is a local flow of energy, at speeds not exceeding the speed of light; from the maximum force $F_{\max} = c^4/(4G)$ [2], the upper limit of the output power is

$$P_{\max} = F_{\max}\, c = \frac{c^5}{4G} \approx 9.1 \times 10^{51}\ \mathrm{W} \tag{25}$$

This upper limit is about 2×10^{25} times the solar luminosity. This upper limit constrains only the energy flow through the throat. The diameter at which the throat opens is only a starting size, which then grows rapidly. At the burst, registration is completed in one step: all relations transfer with the horizons at once into the Hubble sphere of the new universe (Section 4.2); conversion follows a dynamical process: the unpacking of capsule packs and the unfolding of space proceed gradually on the side of the new universe, the bulk of the matter being converted early; the unfolding is not isotropic, the region near the throat unfolding more slowly and remaining denser, and the conversion rate of the remnant is set by the expansion dynamics on the far side of the throat and is lower than the power upper limit of Eq. (25). If the energy to be converted is taken as the matter-capsule energy $N_b E_P$ inherited by the Hubble sphere, the shortest time needed to convert it at $P_{\max}$ is $t_{\min} = N_b E_P / P_{\max} \approx 2.9 \times 10^{17}$ s $\approx 9.1 \times 10^9$ yr. This time is independent of the diameter of the throat opening, which determines only whether the energy flow can start. If the actual power P_{eff} satisfies $P_{\mathrm{eff}} \leq 0.66\, P_{\max}$, the remnant can survive to the present ($t_0 \approx 1.38 \times 10^{10}$ yr, the age of the universe with the burst taken as its starting point) and persist as a long-lived remnant of the parent black hole (its observational signatures are discussed in Section 6.2). The Planck power is far above the power of ordinary astrophysical processes, so $P_{\mathrm{eff}} \ll P_{\max}$ is a reasonable assumption; however, this rate has not been derived from the throat dynamics in this paper, and the conclusions above are therefore conditional. Models in which the interior of a black hole connects to a new universe have precedents in the literature: Frolov, Markov and Mukhanov discussed the interior of a black hole connecting through a transition layer to a de Sitter universe [54], and Popławski discussed a new universe born through a bounce on the other side of a black hole [55].

Creation in the early stage of the burst, and distribution and recombination by code. The early hot state needs a heat source. The background capsules cancel in a zero sum and contribute energy only through the residual, so filling space with them does not by itself provide a temperature; the heat source is the $1+1 \to 2 \to 1$ cycle that occurs continually during rapid creation (Section 3.3): newly created capsules are in contact as soon as they appear, combine in pairs into $N = 2$ black holes and evaporate at once, each round releasing a pack of E_P as radiation; as long as creation continues, the radiation is replenished, forming and maintaining

the early high-temperature environment. The energy of the early hot state therefore comes from the rapid creation of background capsules and not from the capsule packs released by the parent black hole, whose rest mass ($m_b = 2.9 \times 10^{52}$ kg) is far smaller than the energy of the early radiation; radiation energy decreases with redshift in the expansion, $d(\rho_E a^3) = -p\, d(a^3)$, and is not itself conserved. The positive zero-point energy and the negative gravitational energy of the background capsules cancel in a zero sum (Paper II [2]); we propose that after capsules have turned into radiation through the cycle, the negative gravitational energy that balanced them passes into the gravitational field of the expanding universe, its dynamical effect being to slow the local expansion, which nevertheless continues; after the heating period the cycle stops and the local expansion resynchronizes with the global expansion. A quantitative energy account is left to future work. At the burst the registrations on the two horizons transfer together into the Hubble sphere, $S = S_+ + S_- = 4\pi k_B N_b^2$, corresponding to the area $A_+ + A_- = 4A_i$ (Eq. (6)), i.e. a Hubble sphere of radius $2N_b\ell_p$ (Eq. (23)); the outer horizon has only A_+ and cannot hold the registrations of the inner horizon, so the outer horizon must expand into the Hubble sphere. The burst occurs near the existence boundary, where $N_{irr} \approx k \equiv \sqrt{N_b^2 - N_{irr}^2} \approx N_b/\sqrt{2}$ and $S_+ \approx S_- \approx S/2$; the radius of the outer horizon grows from about $\sqrt{2}N_b\ell_p$ to $2N_b\ell_p$, and its area doubles. Before the burst, the interior of the black hole contains only the capsules accumulated by accretion and no background capsules; after the burst, the capsule packs occupy only $1/N_b^2$ of the volume of the Hubble sphere, and the remaining vacancies are filled by background capsules created rapidly at the intrinsic density ρ_c, the number required being N_b^2 times the capsule number of the parent black hole (Eq. (24)); this stage is inflation. The space of the new universe unfolds on the other side of the throat and is not limited by the region occupied by the black hole in the parent universe; once the vacancies are filled, inflation ends, background capsules are replenished with the expansion according to the creation-rate equation, the density staying constant [2], and the universe enters a steady, continuing expansion. This inflation corresponds to inflation in standard cosmology in that the density is unchanged, the volume grows rapidly and energy is created with it; the difference is that in the present framework it corresponds to a definite physical process, and the newly created capsules are fully topologically normalized and contribute to gravity only through the residual [2], so they do not make the region exceed the horizon condition.

During creation, the earliest and most numerous black holes to form are $N = 2$ black holes, most of which evaporate immediately; as the expansion lowers the local density, the characteristic capsule number that just satisfies the criterion increases (Eqs. (12) and (13)), and where local density fluctuations are large enough, larger black holes form one after another; those whose mass exceeds the critical value survive and become the seeds of dark matter. The periods of particularly high formation rate are set by the code, so the surviving primordial black holes are concentrated in the corresponding narrow spectrum. Black holes at the survival limit of 5×10^{11} kg form at about 10^{-24} s, and those in the asteroid-mass window at about 10^{-22}–10^{-17} s, far earlier than nucleosynthesis. This agrees with the crystallization picture of Section 3.3: nuclei precipitate first, and the matter precipitating later gathers around them. After the stage of rapid creation ends, new capsules are replenished only according to the

creation-rate equation, the probability of mutual contact drops sharply, and $N = 2$ black holes stop forming, and the remaining capsules stay as background, thereafter appearing only through the residual; this is also why today's background capsules remain stable.

The capsules released by a black hole and the capsules newly created in the background are physically identical, all being the same E_c [2]; they differ only in relations: the released packs carry the relations registered in the parent black hole, i.e. the organizational code, while the newly created packs do not. The code is not attached to any particular pack but is the relations between packs themselves; the matter and structure of the new universe are therefore not generated at random but unfold entirely by recognition and recombination according to the code: how long the creation stage lasts, what fraction is converted into radiation, how many black holes survive and where celestial bodies form are all decided by the inherited code, and so is the ratio of dark to visible matter. E_c therefore has only three evolutionary pathways, corresponding to dark energy, dark matter and visible matter.

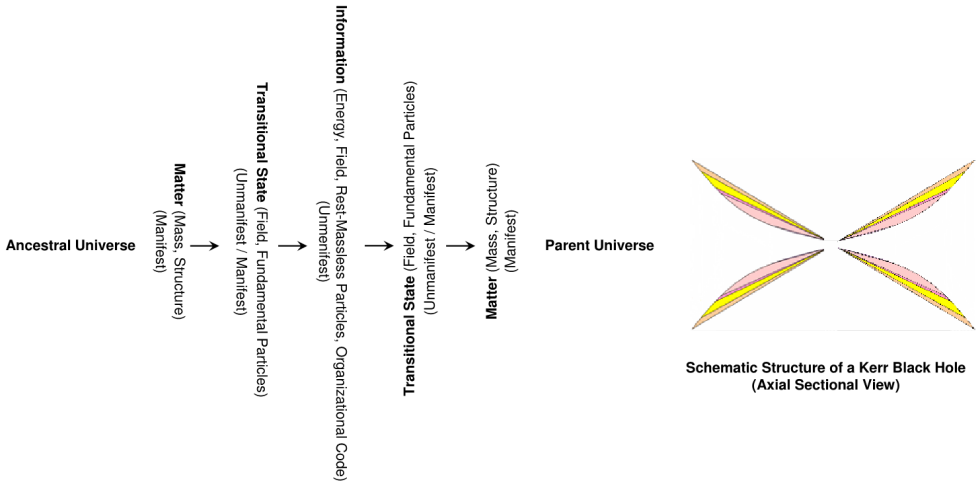

Fig. 6 Schematic diagram of holographic folding and unfolding between implicate and explicate orders of ancestral and parent universes via a Kerr black hole

Figure 6 illustrates the process: matter of the ancestral universe is accreted by the parent black hole and turns from the explicate to the implicate order (packed into capsule packs with relations registered); after the burst, these packs are released on the other side of the throat and, through the transitional state, become manifest again as the matter and structure of the parent universe.

Trigger condition. By the existence criterion [3, 4], the lower limit of the difference of the areal radii of the two horizons is $2\ell_p$: the two horizons register the irreducible part and the rotational part respectively, and when the separation falls below the lower limit the two registrations mix and can no longer be distinguished, and

the structure breaks; the classical extremal point at which the two horizons coincide cannot be reached. Near the existence boundary, the absorption of one more rotational pack takes the separation below the lower limit in one step [4]. The spin of a black hole increases through accretion; the last rotational pack takes the black hole beyond the existence boundary, and the structure breaks and bursts, after which accretion may stop. This is the criterion of the present framework. In classical theory, the radiation torque of thin-disc accretion stops the spin at about 0.998 [56]; this cutoff comes from the accretion environment, not from spacetime itself; how a cosmic egg cell gets past it to reach the existence boundary is listed as an open question (Section 8.2).

4.4 The three-in-one mechanism of intergenerational cosmic reproduction

The black hole, as an "unborn cosmic egg cell", possesses, in a single physical entity, the organizational functions embodied in the three modes of reproduction in biology:

Viviparity: maternal nourishment by the equatorial accretion disc. The core of viviparity is that the embryo draws nourishment from the mother through the placenta and umbilical cord. An active supermassive black hole is surrounded in its equatorial plane by a huge accretion disc; gas, torn-apart stars and radiation of the parent universe flow in continuously through this "cosmic placenta", are packed at the inner interface R_i and registered on the horizon, accumulate mass–energy for the child universe, and supplement the pre-set organizational code with a small number of registrations.

Ovoviviparity: isolated incubation within the horizon. In ovoviviparity the embryo develops inside the mother but is wrapped in an independent egg membrane. After matter crosses the horizon it enters a region causally isolated from the outside; the outside can still feed matter and disturbances inwards but cannot read or control the internal relational states already formed, showing the features of "isolation by the eggshell + protection by the mother".

Oviparity: independent hatching and the burst. The end point of oviparity is leaving the mother and hatching independently. Only supermassive black holes can take the role of cosmic egg cells, such as TON 618, Phoenix A and Holm 15A at the centres of giant galaxies; at the burst, all relations transfer in one step with the horizons, and the capsule packs are released gradually on the side of the new universe and unfold according to the code into a new universe.

Biological examples of the three reproductive strategies and the three-generation nesting are given in Paper I [1].

4.5 Transgenerational pre-setting in cosmic evolution

Paper I defined transgenerational germline pre-setting as follows: while the grandparent generation supports the embryonic development of the parent generation, the source of organizational information of the child generation is already established at the same time, forming a recursive organization of three continuously nested generations [1]. In humans, for example, by about the 5th–6th month of gestation the ovaries of a female fetus already contain millions of primary oocytes, so that one pregnancy

already links three generations, grandparent, parent and child; the specification and migration of primordial germ cells and the formation of primordial follicles, and the argument for why transgenerational pre-setting is necessary (to avoid the accumulation of organizational noise from reverse compression in the mature individual), are given in Paper I [1]. On the cosmic side, the continuing support of the grandparent generation is realized by the common E_c background: the rapid creation of the parent universe and the continuing creation of capsules thereafter both come from this background shared by all generations, while the matter accreted by child black holes is supplied entirely by the parent universe.

Correspondingly, the organizational code of the parent black hole was pre-set when it formed as a primordial black hole: it formed after the burst of the ancestral black hole, before about the electroweak phase transition ($t \approx 10^{-12}$ s). The relations registered at this stage form the functional core of the code of the parent universe but only a tiny fraction of it in number: by Eq. (13), the characteristic mass formed at $t \approx 10^{-12}$ s is about 4.0×10^{23} kg (about 7% of the Earth's mass), whereas the parent black hole at the burst is about 2.9×10^{52} kg, so the early relations make up a fraction $N_0^2/N_b^2 \sim 2 \times 10^{-58}$ of all relations. This is the same as for a fertilized egg: the initial state has a mass far smaller than the mature individual, yet its organizational information governs later development. Thereafter the parent black hole kept accreting in the ancestral universe; the accreted matter was likewise packed and registered in order, but served mainly to accumulate mass–energy for the parent black hole itself; a small number of registrations recorded the adaptation of the parent generation to its environment in the ancestral universe and are passed on with the code from generation to generation, until the black hole crosses the existence boundary and bursts. The code that the parent black hole inherited from the ancestral universe determines the initial distribution of matter and the formation of structure in the parent universe. As Fig. 5 shows, since the two generations of universes are connected by a black hole and are originally one, this pre-setting is not a transfer of information between two independent systems but the natural inheritance of internal states within one continuing system.

In our parent universe, child black holes (future cosmic egg cells) also start as primordial black holes. They must complete their pre-setting before the large-scale hierarchical organization of explicate-order matter begins; we take the electroweak phase transition after the burst of the parent black hole ($t \approx 10^{-12}$ s, when elementary particles acquire rest mass) as this time limit. Those that survive have masses not less than 5×10^{11} kg. Thereafter child black holes develop together with the "cells, tissues and organs" of the parent universe: star clusters and giant molecular clouds correspond to tissues of the parent universe and complete galaxies to its organs, until one of the child black holes triggers the next burst.

4.6 Relation to Smolin's hypothesis of cosmological natural selection

Smolin proposed the hypothesis of cosmological natural selection [9]: when a star collapses into a black hole, the singularity inside "bounces" and gives birth to a new universe on the other side of spacetime, which inherits the physical constants of the

mother universe with small variations. This is structurally in line with the view of this paper that "our universe was gestated by the parent black hole". Smolin's hypothesis, however, does not say by what concrete mechanism a black hole performs this "selection" and "inheritance". What this paper gives is an organizational extension of the hypothesis: what is inherited is the relations registered in order inside the black hole (the organizational code); the mode of inheritance is the transfer of the relations as a whole at the burst (Section 4.3); and the channel of inheritance is the three-in-one structure of viviparity, ovoviviparity and oviparity (Section 4.4). How later registrations influence the physical parameters of the next generation has no quantitative mapping yet, so this is not yet a complete mechanism of heredity. The two can be regarded as complementary rather than competing views.

5 Dark energy, dark matter and visible matter: the three evolutionary pathways of the capsule E_c

5.1 Three evolutionary pathways

Observations by the Planck satellite give, for the present total energy density of the universe, about 68.5% dark energy, about 26.5% dark matter and about 4.9% visible (baryonic) matter [57]. The physical origins of the three have mostly been treated separately, without a unifying mechanism connecting them.

By Sections 4.2 and 4.3, all the capsule packs are released as a whole when the parent black hole bursts. A single E_c can neither pack nor unpack by itself (Section 3.1), so E_c has only three evolutionary pathways, corresponding to the three components of the universe:

1. remaining a free E_c and forming the cosmic background, i.e. dark energy. This background is shared by all generations of universes, and the packs that stay free at the release join it; dark energy comes mainly from the common background, not from the distribution of the present release;
2. re-clustering into black holes where the density reaches ρ_c/N^2, i.e. dark matter;
3. being unpacked into radiation, which condenses into particles, atoms and celestial bodies, i.e. visible matter.

What the burst distributes is only matter: the N_b released packs are divided by the organizational code into dark and visible matter, and the dark-matter part clusters preferentially at the highest density. This ratio can at present only be determined from observation and has not yet been derived from the code. After the distribution, accretion slowly converts visible matter into capsule packs, i.e. into dark matter, with losses: accretion radiation carries away about 6% (Schwarzschild) to 42% (extremal Kerr) of the rest mass, stellar nuclear fusion about 0.7%, and the gravitational waves of black-hole mergers about 5% (about $3M_\odot/65M_\odot$ in GW150914). This conversion is still small: the mass density of supermassive black holes today is only about 10^{-4} of the baryon density [58], and the total mass of stellar-mass black holes is only about 0.2% of the baryons [59], so the ratio of dark matter to baryons at recombination given by Planck, $\Omega_c h^2/\Omega_b h^2 = 0.120/0.0224 \approx 5.4$ [57] (Ω_c and Ω_b are the density

parameters of dark matter and baryons, and h is H_0 in units of 100 $\mathrm{km\,s^{-1}\,Mpc^{-1}}$), is essentially unchanged to the present. This ratio reflects mainly the distribution at the burst, together with possible cross-generational black holes (left over from the parent or even earlier generations); the shares of the two cannot at present be separated, so it can serve only as a reference for the distribution at the burst. The dark-energy density does not dilute with the expansion ($w = -1$), while the matter density is inversely proportional to the cube of the cosmic scale factor, so the ratio of dark energy to matter changes with the age of the universe, and today's roughly 68.5%:31.5% is only a cross-section at the present moment. Most black holes in a universe stay in their own generation and only very few reach the burst point; the cross-generational mass–energy budget is not discussed in this paper.

5.2 Dark energy: the free E_c background

Dark energy corresponds to the free E_c in the cosmic background. According to Paper II, the positive zero-point energy and the negative gravitational energy of the background capsules cancel in a zero sum, so that as a whole they are not a macroscopic source of gravity; the two normalization paths, the gravitational mass–energy limit (route B) and the quantum zero-point field (route C), give the same energy scale at the capsule scale, and the measured dark-energy density is the residual potential relative to this symmetric point ($\rho_c^B = \rho_c^C$) [2]:

$$\rho_{obs} = \frac{\Omega_\Lambda}{N_{\mathcal{H}}^2}\,\rho_c c^2 = \delta_c\,\rho_c c^2 \approx 5.25 \times 10^{-10}\ \mathrm{J/m^3}, \qquad \delta_c \approx 3.8 \times 10^{-122} \tag{26}$$

The residual coefficient and the mean black-hole density obey the same $1/N^2$ law (Eq. (8)), with N replaced by the capsule number $N_{\mathcal{H}}$ of the Hubble sphere. Ω_Λ and $N_{\mathcal{H}}$ both evolve with the universe, but in their combination H cancels, $\delta_c = \Omega_\Lambda/N_{\mathcal{H}}^2 = \rho_\Lambda/\rho_c$, which depends only on the dark-energy density itself; in the simplest form δ_c is constant, and the residual potential does not decrease as $N_{\mathcal{H}}$ grows. The background capsules are replenished according to the creation-rate equation as the universe expands, the density staying constant and the equation of state being $w = -1$ [2]; dark energy with $w = -1$ is accreted by black holes at zero rate [60], and a growing black hole merely pushes aside the E_c of the background [3]. If DESI and other observations confirm that $w(z)$ evolves with time [12, 13], then δ_c varies correspondingly with time, $w = -1 - \dot{\delta}_c/(3H\delta_c)$ (Paper II [2]), which will be a direct test of the picture.

5.3 Dark matter: capsule packs in black holes

Dark matter corresponds to the E_c that exist as capsule packs inside all black holes: from primordial black holes re-clustered after the burst where the code specifies, through black holes formed by stellar collapse (Eq. (10)), to supermassive black holes grown by accretion and mergers. The first two form by the same criterion and the last grow from them; all three have the same final structure and are hard to distinguish by their gravitational effects. Black holes in non-accreting, non-merging phases

are electromagnetically silent and show themselves only through gravity, in accordance with the observed properties of dark matter. The gravitational skeleton of the large-scale structure of the universe consists of clustered black holes (i.e. dark matter, Section 3.6), and visible matter settles along this skeleton (Section 5.4).

5.4 Visible matter and cosmic voids

Visible matter corresponds to unpacked energy: unpacking releases it as radiation, which cools and condenses into elementary particles and atoms, and further into stars, planets and life. This part of the baryonic matter, outside black holes and between black-hole units, can be likened to the "extracellular matrix" of black holes.

Visible matter settles along the dark-matter skeleton, and under the combined action of gravitational aggregation and background unfolding the large-scale structure of the universe differentiates into high-density galaxies, galaxy clusters and filaments, and the low-density cosmic voids between them [61]. Voids are not "nothingness" but complementary regions formed naturally by the same unfolding process: where explicate-order matter has receded, the free E_c background is not screened, the gravity of matter is weaker, and the unfolding action of the background is expressed relatively more fully. By Paper I, the continuous functional environment P_e in a bundle-type organization is shared by several subdomains [1]; in the universe, galaxies, clusters and filaments are recursive organizational units, the free E_c background is the continuous environment they share, and voids are where this background shows through at low matter density, not independent organizational domains. This picture is discussed in detail in Section 6 of Paper II [2].

5.5 Implicate and explicate order: two readings of the same set of relations

According to Bohm's ontological framework [18, 19], the explicate order of the universe is rooted in an implicate order with pre-spacetime character; this mechanism of enfolding and unfolding was further characterized with process algebra by Lohrey and Boreham [62] and extended by Torday to biological evolution and to the topological boundary analysis of the gravitational field [63].

Paper III gave the quantitative meaning of this pair of concepts for black holes [3]. Let X be the configuration of relations inside the horizon and Y the information held by an observer; in the information-theoretic identity $H(X) = H(X|Y) + I(X;Y)$, $H(X)$ corresponds to the total relational entropy of the black hole, $S = S_+ + S_- = 4\pi k_B N^2$ (in the Schwarzschild case S_{BH}). Here $H(X)$, $H(X|Y)$ and $I(X;Y)$ are dimensionless information measures expressed in nats, with the thermodynamic entropy normalized by k_B: $H(X) = S/k_B = 4\pi N^2$; conversion to bits requires a further division by $\ln 2$. An external observer can, by the no-hair theorem, measure only the mass, angular momentum and charge, so $I(X;Y) = 0$ and $H(X|Y) = S/k_B$: the black hole appears completely disordered, i.e. as Hawking thermal radiation; from the internal structure, the relations are completely fixed by the packing order, $H(X|Y) = 0$ and $I(X;Y) = S/k_B$: it appears completely ordered. "Maximal black-hole entropy means maximal disorder" and "all relations established means maximal

order" are the external and internal readings of the same number. In bits, by Eq. (2), $I_{\mathrm{BH}} = S/(k_B \ln 2)$ splits into two parts: $H(X|Y)/\ln 2$ is the part unknown to the observer and appears as entropy, and $I(X;Y)/\ln 2$ is the known part and appears as information. $I(X;Y)$ corresponds to the degree of order seen by the observer and $H(X|Y)$ to the degree of disorder; information and entropy are the ordered and disordered readings of the same total I_{BH}. The identity can also be written $I(X;Y) = S/k_B - H(X|Y)$: the information gained equals the deficit of entropy, which is Brillouin's negentropy principle [64, 65]. For a Kerr black hole, this total $4\pi k_B N^2$ is distributed over the two horizons: the outer-horizon entropy S_+ corresponds to the surface information Ψ_s and the inner-horizon entropy S_- to the bulk information Ψ_b (Eq. (7)).

Two kinds of hidden–manifest conversion must be distinguished here. At the epistemic level, the same configuration of relations is knowable to different degrees by different observers, i.e. the division between conditional entropy and mutual information; at the organizational level, registered relations form material structure through unpacking and recursive organization. The two are related but not equivalent: an external observer obtaining information about the interior of a black hole does not mean that the capsules inside have been unpacked, and the manifestation of material structure does not mean that an observer holds all of its organizational information.

Accordingly, we define the implicate and explicate orders, in the course of black-hole evolution, as two readings of the same set of relations: the implicate order is the internal reading, in which the relations are fully established but not manifest outside; the explicate order is the external reading, in which the relations, through unpacking and unfolding, become manifest as matter and structure. The unfolding of the universe can thus be summarized as

$$\begin{array}{c}\text{implicate order}\\(\text{relations registered}\\\text{in the black hole})\end{array} \xrightarrow[\text{recombination by code}]{\text{burst}} \begin{array}{c}\text{explicate order}\\(\text{matter and structure}\\\text{of the new universe})\end{array} \tag{27}$$

The same correspondence exists in biological systems: the genome of the embryo is the implicate order, and individual development is its manifestation [1]. Living organisms are not imitating black holes; the two follow the same set of organizing principles.

6 CMB anomalies and the ancestral–parent–child "three generations in one frame"

According to traditional inflationary models, inflation smooths out pre-existing inhomogeneities of the early universe while generating nearly Gaussian primordial perturbations, and the CMB should be a statistically isotropic Gaussian random field; several statistical anomalies have, however, been observed. We regard the axis of evil among them as an imprint left by the ancestral universe and the Cold Spot as the remnant of the parent black hole; child black holes are normal objects, and parallel black holes may also be among the supermassive black holes visible today (Section 6.4). The three belong to three generations yet can appear in the same all-sky map, forming

"three generations in one frame" (for the intergenerational relations see Sections 4.2 and 4.5).

6.1 The axis of evil: imprint of the ancestral universe

The CMB "axis of evil", i.e. the strong alignment of the quadrupole ($l = 2$) and octopole ($l = 3$) over the whole sky, is a global signal rather than a locally identifiable patch [66–68]. We regard it as an imprint left by the ancestral universe: it formed before the stage of rapid creation and was stretched during that stage to cover almost the whole celestial sphere, running through the entire observable universe. Our universe inherited the primordial angular momentum left by the ancestral generation, so the spin axes of the black holes of every generation are "locked" near the principal axis of the ancestral generation. Other explanations of this anomaly exist in the literature, and we acknowledge this plainly; but the Cold Spot and the axis of evil are robust as observed anomalies.

The "axis locking" meant here is not the collinearity of spin axes on the scale of the Solar System but the cross-generational inheritance of axis direction among the ancestral, parent and child black holes; local events involving small bodies are not enough to change the inherited global principal axis. Figure 5 gives a geometric sketch of axis locking: the throats and jet directions of the ancestral (G1), parent (G2) and child (G3) generations lie roughly along one axis, and the off-centre directions of the nested layers are also along this axis. For simplicity the figure draws the axes of the three generations on one straight line; in reality the black holes of each generation undergo accretion and mergers as they grow, and their angular momentum is perturbed, so the axes of the generations are not strictly collinear, but the deviations are small. From the direction of the axis of evil, $(l, b) \approx (260°, 60°)$ [67], and that of the CMB dipole, $(264.0°, 48.3°)$ [69], the angle between the two axes is about 12° (for undirected axes, $\theta = \arccos|\hat{n}_1 \cdot \hat{n}_2|$): close but not coincident, which belongs to this case. We therefore predict that the statistical distribution of the spin axes and jet directions of the child supermassive black holes of our universe should be biased towards this principal axis. This prediction can be tested with the orientational order parameter $Q = \langle P_2(\cos\theta)\rangle = \langle(3\cos^2\theta - 1)/2\rangle$ [70], where θ is the angle between the spin axis of a black hole and the principal axis. For an isotropic distribution $\langle\cos^2\theta\rangle = 1/3$ and $Q = 0$; for all axes parallel or antiparallel $Q = 1$, and for all axes perpendicular $Q = -1/2$. The CMB dipole arises mainly from the motion of the observer relative to the CMB rest frame, and relating it to the cross-generational axis is an additional interpretation of this paper. There are already related clues in the literature, such as the large-scale alignment of quasar polarization directions on Gpc scales [71, 72] and the large-scale alignment of radio-galaxy jet directions [73]; the origins of these results are still disputed, and we list them only as testable directions.

6.2 The Cold Spot: remnant of the parent black hole

We regard the CMB Cold Spot as the remnant of the parent black hole. After the parent black hole burst, the region near the throat (the throat on the right of G2 in Fig. 5) retained the most concentrated debris of matter; the region after the burst

can be countless times larger than before, and the debris was magnified accordingly to cosmological scales. The Cold Spot formed after the stage of rapid creation and was not stretched by that stage, so it remains local.

The existence of the Cold Spot has been confirmed independently in WMAP and Planck data [66, 74–77]: its radius on the sky is about 5°–10°, its core is about 70–150 μK colder than the background, and it is surrounded by a ring about 20–30 μK warmer than the background, whereas on the filtering scale of the Cold Spot the standard fluctuations of the background are only about ± 18 μK. Its overall statistical significance depends on the method and filtering scale used and is roughly 2–3σ; the dispute concerns its significance and physical origin, not its existence. Before filtering the core was once described as four sub-blobs [74], but by their values only one extremum centre is truly significant, consistent with the later treatment by Cruz et al., who smoothed it into a single cold spot. Other explanations of its origin exist, such as statistical fluctuation, foreground contamination, a supervoid and a cosmic texture [77], and we acknowledge this plainly.

In the picture of this paper, the low temperature of the Cold Spot core has the gravitational potential well as its main mechanism, with two further possible contributions. The debris, as a region of concentrated mass, forms a deeper gravitational potential well: if the well lies near the last-scattering surface, the redshift of photons climbing out of it exceeds their intrinsic excess heat, so that more mass appears colder (the Sachs–Wolfe effect); if it lies between the last-scattering surface and the observer, the blueshift on entering and the redshift on leaving a static well cancel, and the net effect comes from the evolution of the well with time (the integrated Sachs–Wolfe effect). In addition, the remnant itself hardly radiates and absorbs the photons falling on it, leaving a "photon-deficient" shadow, whose strength and frequency dependence depend on the absorption cross-section and optical depth of the remnant. In the early stage of the burst the region near the throat expanded less and was denser, and the surrounding regions that expanded more may also have drawn heat away from it, forming a compensated structure with a cold core and a warm outer ring; this, however, requires an additional energy-transport mechanism, whose thermodynamic basis remains to be established. That the Cold Spot is nearly circular and concentric on the celestial sphere also agrees with the picture of a three-dimensional debris potential well, symmetric about the spin axis, intersecting the last-scattering surface.

Distinguishing from the supervoid explanation. The other main explanation attributes the Cold Spot to a supervoid along the line of sight [77, 78]. The two can be distinguished by the CMB lensing signal: the remnant and debris potential well of this paper predict a mass excess in the direction of the Cold Spot, whereas the supervoid explanation predicts a mass deficit, and the lensing signals of the two have opposite signs. This test requires the remnant to lie in front of the background light source, the three-dimensional position of the remnant being a necessary condition; it does not depend on the full dynamics of the burst: as long as the remnant has an observable positive projected mass excess, it can be distinguished from the supervoid explanation.

6.3 The scale hierarchy of three generations in one frame

The older the generation, the more expansion its relic has undergone, and the larger its angular scale and the more diluted its amplitude: the imprint of the ancestral universe is at about 60°–90° ($l = 2, 3$), the remnant of the parent black hole (the Cold Spot) at about 5°–10°, and child black holes are point sources on the sky; this scale hierarchy agrees with the generational picture: the axis of evil and the Cold Spot are both imprinted on the last-scattering surface at the same distance, and the expansion of the universe is global and stretches both in the same proportion, so the ratio of their angular scales directly reflects the ratio of their comoving scales; the two differ by about an order of magnitude, which ordinary differences in physical size cannot overturn. Child black holes are point sources on the sky, and their place in the hierarchy is equally clear. This hierarchy corresponds to the nesting of the generations (Fig. 5): the outer layer leaves only a weak imprint on the largest scales; the layers are not concentric, and we are in an off-centre position relative to the outer layer, which gives a preferred direction on the largest scales, in accordance with the directionality of the axis of evil and of the north–south hemispherical power asymmetry. The axis of evil (ancestral), the Cold Spot (parent) and the visible supermassive black holes (child) can appear at the same time in the same all-sky map, constituting in principle the observational clue of "three generations in one frame". It should be noted that the statistical significance of the axis of evil and of the Cold Spot is each about 2–3σ and both are disputed; "three generations in one frame" is a hypothetical framework proposed in this paper, and the observations above only provide clues for it and are not sufficient on their own to confirm its specific mechanism.

The closest precedent is the "Hawking points" of Penrose's conformal cyclic cosmology: An, Meissner, Nurowski and Penrose reported a set of anomalous hot spots in the CMB and interpreted them as imprints of the energy of black holes evaporated in a previous aeon [79]; Jow and Scott re-evaluated them and found them statistically insignificant [80]. The difference from the present paper is that in conformal cyclic cosmology the aeons follow one another and the relics are hot spots produced by the energy of evaporated black holes, whereas here the generations coexist in a nested manner, the Cold Spot comes from a debris potential well, and there is a scale hierarchy over three generations.

6.4 Parallel black holes

Figure 5 shows only a single-line schematic of three generations, whereas every generation of universe contains a large number of supermassive black holes. The Hubble sphere of the parent universe imposes no binding on unburst parent black holes, so some of them fall inside the Hubble sphere of the parent universe and can be seen by its observers. Together with child primordial black holes and child collapsed black holes, three classes of black holes may coexist inside the Hubble sphere: child primordial black holes, formed by the density criterion in the early high-density phase of their own generation, whose surviving masses start from 5×10^{11} kg and are concentrated in a narrow mass window; child collapsed black holes, formed by the collapse of stars whose mass exceeds the TOV limit (Section 3.2); and parallel black holes, which

are unburst parent black holes that fall into the Hubble sphere and whose horizons remain binding before the burst (Section 4.2).

The difference between primordial and collapsed black holes lies in the epoch of their formation criterion and in the number of capsules (Sections 3.2 and 3). The formation history of a parallel black hole does not depend on the present parent universe, so its growth history can be longer than the age of this universe.

Observationally, some early supermassive black holes have masses that are out of proportion to the evolutionary stage of their host galaxies. The direct dynamical mass of Abell 2744-QSO1 at redshift 7.04 is about $5 \times 10^7\, M_\odot$, its host stellar mass is less than half that of the black hole, and the gas around it has a chemical composition close to primordial [81]. Some of the little red dots (LRDs) also show features of accretion by massive black holes, yet the organization of their host galaxies is out of proportion to the black-hole mass [82]. Within this framework these observations can be explained by parallel black holes; they can also be explained by rapid accretion or direct collapse of primordial black holes [83]. They are therefore, for now, only a qualitative, testable expectation.

6.5 Partition of the break-point angular momentum and its association with the spin direction of celestial bodies (conjecture)

At the break point the black hole has $\chi \to 1$ and final-state angular momentum $J = N_b^2\hbar$, where N_b is the total number of capsules of the black hole in its final state, defined in Eqs. (23) and (24). After the break the outer horizon turns into the Hubble sphere, the capsule packs inside the parent black hole are released, and this angular momentum is transferred into the Hubble sphere with the released packs, becoming the initial state of the Hubble sphere. This section concerns the angular momentum carried by the released capsule packs.

The total released angular momentum $N_b^2\hbar$ must satisfy the constraint that the net angular momentum of the Hubble sphere is zero. The overall rotation compatible with this constraint is quoted as $\sim 10^{-9}$ rad/yr for shear-free rigid rotation of the flat ΛCDM universe [84], and as $\sim 10^{-13}$ rad/yr for another model estimate [85]. These two literature values, in rad/yr, are quoted only to compare orders of magnitude and do not enter the derivation. The constraint requires an output term $-N_b^2\hbar$ not contained in the Hubble sphere; its mechanism is not yet determined and is used here only as a constraint.

The partition of the released angular momentum is derived in Paper IV [4] and is used here directly: Eq. (76) there relates the Hubble-sphere packets J_+^H and J_-^H to the black-hole-state magnitudes, Eq. (77) is the zero-sum condition, Eq. (78) is the normalization, and Eq. (79) gives the two packets equal magnitudes, each $\frac{1}{2}N_b^2\hbar$. The fractions of the two packets' angular momentum at the break point are therefore

$$\frac{|J_+^H|}{N_b^2\hbar} = \tfrac{1}{2} = 50\%, \qquad \frac{|J_-^H|}{N_b^2\hbar} = \tfrac{1}{2} = 50\%, \tag{28}$$

which are the initial values of the Hubble-sphere packets at the break point, given directly by Eq. (79) of Paper IV. The two packets have opposite signs, and this relation does not depend on the observer; which packet is clockwise depends on the observing position and is therefore arbitrary.

If the zero net angular momentum of the Hubble sphere is taken as the constraint after the break, then whatever the ratio of the two parts before the break, 20:80, 30:70 or 29.3:70.7, renormalization gives two oppositely rotating classes each carrying 50% of the angular momentum. This forms a zero-sum initial state, a statistically nearly balanced initial distribution of rotation whose spatial distribution is not yet determined. The constraint fixes only the global partition of angular momentum; the packets may nevertheless form local rotational biases of varying degree. Whether the initial spatial distribution is random, and how it evolves into the spin statistics of later celestial bodies, remain to be studied.

After release, the packs go to the two destinations of Section 5.1: one part materializes as celestial matter and radiation, and the other part re-clusters into next-generation black holes. The free capsules of the background constitute dark energy, do not take part in the release, and are not counted here. How the released angular momentum is divided between the two destinations, and how the angular momentum of the newly formed black holes is accounted, is not given by the framework at present and is left as an open question. How the macroscopic angular momentum of the parent black hole is converted, during the break, into the two oppositely signed initial Hubble-sphere parts is likewise not yet determined. How later celestial bodies form and acquire orbital angular momentum lies outside the scope of this initial-state derivation.

After the break the Hubble sphere has no binding force. As it expands, some parallel black holes and parallel celestial bodies are taken in, radiation also flows out, and the formation, mergers and disappearance of celestial bodies all change the ratio of the two classes of angular momentum. The fractions in Eq. (28) are therefore the initial values of the Hubble sphere; the present ratio is the result of about 13.8 Gyr of evolution, and the initial fractions are not to be compared directly with present-day values. As examples of present-day values, the merged sample of 958,841 galaxies contains 479,663 clockwise and 479,178 counterclockwise galaxies [86]; the local asymmetries are of order one to three percent [86]; and in the high-redshift JADES sample, relative to the Milky Way, there are 158 clockwise and 105 counterclockwise galaxies [87].

7 Deconstruction, information conservation and the cross-scale mapping of three-level mechanisms of inheritance

7.1 A common organizing principle and the differentiation of reproductive strategies

The correspondence between the three modes of reproduction and black-hole geometry was given in Section 4.4; here we add its meaning in temporal order. In a linear view of time, black holes came first and animals appeared ten billion years later, so

oviparity, viviparity and ovoviviparity are often regarded as independent inventions of carbon-based life under environmental pressure; this paper takes a different view. From the standpoint of unified recursive organizational theory, the structure around a supermassive black hole is the most primordial realization of the same organizing principle in the inorganic physical world; after carbon-based life arose, the environmental constraints of specific ecological niches led different groups of organisms to differentiate different modes of reproduction, a realization of structural recurrence and structural recursion under different environments (for the three-generation nesting under the three modes see Paper I [1]). Living organisms are not imitating black holes; they follow the same set of organizing principles together with black holes.

7.2 Deconstruction and information conservation

The biological side. At cell division, structural organelles such as the endoplasmic reticulum and the Golgi apparatus are not passed on intact but disassemble into seeds of structural organelles, which are redistributed during division and rebuilt in the daughter cells; the genetic information is replicated with high fidelity during the S phase of interphase; after entry into division the nuclear envelope disassembles into small vesicles in prophase, and the chromosomes are segregated with high fidelity during mitosis [1]. What is inherited is not only nuclear DNA but also organelle seeds, cytoplasmic components and epigenetic states, i.e. the unified organizational information $\Psi(SS)$ of Paper I [1]. What is deconstructed is macroscopic structure; what is kept is organizational information.

The black-hole side. The macroscopic structures of the parent universe likewise do not enter the child universe in their original form. Galaxies, stars and molecules falling into a black hole are torn apart by tidal forces near the horizon, first decomposed into energy shares matched to the temperature at the time, and then packed at the inner interface R_i into E_c packs, which are registered in order on the horizon [3]. What is deconstructed is macroscopic structure; what is kept is the relations: each pack brings in one self term and $2N$ ordered relations between it and the packs inside the horizon, and the packing order records the history of the black hole completely. Relational capacity and organizational code must be distinguished. Two black holes with the same N both have N^2 relations, but with different accretion histories the registered content differs, much as genomes with the same number of bases can differ in sequence. We write the relational code of a black hole as $K_N = \{q_{ij} \mid i, j = 1, \ldots, N\}$, where q_{ii} is the registration state of a self term and q_{ij} that of the ordered relation between the ith and jth capsules; the number of matrix elements is exactly N^2, and no relational terms are added. N^2 is the registration capacity, and K_N the concrete organizational code.

The interior of a black hole neither "removes" information nor lowers its entropy: the total amount of relations is conserved in evaporation and mergers [3]; the difference between the external and internal readings is given in Section 5.5. The so-called "denoising" means that the details of macroscopic structure are deconstructed into uniform capsule packs, while the organizational code is kept completely in the form of the packing order. Paper I argued why biological systems must pre-set the source of organizational information of the next generation at the initial node rather than rely

on reverse compression from the mature individual [1]; the cosmic counterpart is that the core of the organizational code of the child universe is already pre-set when the child black hole forms; the many registrations during accretion mainly serve mass–energy organization and historical record, and only particular parts take part in the adaptive updating of the core code (Section 4.5), rather than being extracted ad hoc from the macroscopic structures of the parent universe at the burst.

It is worth noting that research on the black-hole information problem has always insisted on information conservation, starting from the unitarity of quantum mechanics and not for the sake of inheritance. But once information conservation and "black holes give birth to new universes" hold together [9, 54, 55], the organizational information still retained by a black hole at its burst can neither disappear nor stay in the original black-hole structure, and can only be passed on with the burst to the next-generation universe; in normal evaporation, information is released with the radiation [3]. The black hole is therefore objectively in the position of the gene: it stores and transmits the organizational code. Smolin's hypothesis of cosmological natural selection already uses the language of "inheritance and variation" [9]; what this paper gives is the concrete content of the inheritance: the relations registered in packing order.

The intergenerational generation of universes can thus be summarized as: deconstruction of the material structures of the parent generation → packing and registration (becoming implicate) → transfer of the relations as a whole at the burst → unfolding according to the code (becoming explicate) → recurrence of the material structures of the child generation.

New structures form continually throughout evolution, and the code is not transferred only once at the burst: each new structure arises recursively from existing structures and carries the complete code, expressing different parts of it. The complete code here means the common organizing rules, not a copy of the entire microscopic history of the parent universe in every subunit; three levels must be distinguished: the generative rules inherited in common by all units, the local relational state of the present unit, and the overall relational network formed by all units, just as a cell retains the potential to form a complete individual without containing all the physical states of the mother's lifetime. This is the manifestation of recursive holographic unfolding [1] on cosmic scales.

7.3 Three-level mechanisms of response and inheritance

To maintain present stability in a turbulent environment and at the same time achieve accurate transmission across generations, isomorphic three-level mechanisms exist on biological and cosmic scales.

Long-term mechanism: transgenerational pre-setting. Biological side: the pre-setting of primary oocytes is completed early in the embryo, limiting the transmission of somatic mutations to the next generation, and high-fidelity inheritance is achieved through DNA repair and the germ-plasm barrier [1]. Cosmic side: primordial black holes are pre-set as the oocytes of the child universe (Section 4.5). As in biology, the universe also has a somatic line and a germ line: most black holes in a universe stay in their own generation and form the dark-matter skeleton, corresponding

to somatic cells; only very few reach the burst point and unfold into new universes, corresponding to germ cells.

Medium-term mechanism: epigenetic packaging and adaptive fine-tuning. Biological side: the parent generation can convert environmental stress into epigenetic changes in the germ line (DNA methylation, histone modification and small RNAs), which can escape embryonic reprogramming, be inherited across generations, and make rapid adaptive "fine-tuning" to the environment [88]. Cosmic side: when matter of the parent galaxy falls into a supermassive black hole, its composition, angular momentum and evolutionary history enter the registration with the packing order; we conjecture that this later-registered information may influence the direction of fine-tuning of the physical parameters of the child universe. This conjecture has no quantitative formulation at present.

Short-term mechanism: redundancy and immune defence. Biological side: paired organs, multiple gene copies, heat-shock proteins and the immune system provide immediate stress response and load clearance; the division of labour between redundancy and asymmetric renewal in maintaining organizational continuity is given in Paper I [1]. Cosmic side: clustered black holes (dark-matter haloes, Section 5.3) provide redundancy of the gravitational skeleton, so that the disruption of a local stellar system does not bring down the whole galactic network; when a supermassive black hole is overloaded by accretion, the accretion disc throws off excess mass–energy through the release of angular momentum and bipolar relativistic jets, achieving dynamic load balancing.

8 Conclusions, limitations and outlook

8.1 Main conclusions

Building on Paper I, *Unified Recursive Organization Theory*, Paper II, *The $2d_m$ Minimum Topological Structural Unit*, Paper III, *Relational Structure of the Bekenstein–Hawking Entropy*, and Paper IV, *Angular-Momentum Spectrum of Kerr Black Holes*, this paper maps the biological holography of Paper I to cosmic scales. The main conclusions belong to three levels: quantitative relations derived in the previous papers and in this paper (the formation criterion, the density clock, the critical mass, the existence criterion); the organizational mapping between biology and the cosmos; and new physical hypotheses awaiting test (black-hole bursts, the conversion of the horizons into the Hubble sphere, three generations in one frame). They are as follows.

1. **The unified density criterion for black-hole formation.** A region whose energy is NE_P and whose density reaches ρ_c/N^2 ($\rho_c \approx 1.54 \times 10^{95}$ kg/m^3) forms a black hole of N capsules. Two E_c in contact combine into an $N = 2$ black hole, a special transitional case between packing and unpacking; the density clock expressed in the local density gives $N = t/t_P$ without recourse to the Hubble horizon; at the TOV limit of 2.2–2.3 $M_\odot$ the required mean density is about (3.5–3.8) $\times 10^{18}$ kg/m^3, comparable to the central density of neutron stars. Primordial and stellar-collapse black holes are the same criterion satisfied at different densities and different N.

2. **The survival condition of early black holes.** The critical mass at which the Hawking temperature equals the background temperature, $M_{crit}(t) \propto t^{1/2}$, plays the role of the "critical nucleus": the earliest $N = 2$ seeds evaporate within about 10^{-40} s; only black holes of mass $\gtrsim 5 \times 10^{11}$ kg, i.e. formed where the local density is below about 2.9×10^{56} kg/m^3, survive to the present. The negative heat capacity of black holes makes the larger absorb and the smaller evaporate, isomorphic to Ostwald ripening [33].
3. **Black-hole cores inside celestial bodies.** A black hole able to dominate star formation must approach the Jeans mass, i.e. the order of a solar mass, and forms an accreting black hole rather than an ordinary star; low-mass primordial black holes can only be engulfed passively. If dark matter consists of black holes, Population III stars are rather likely to contain black-hole cores [34], while present-day ordinary stars are very unlikely to contain one [35].
4. **The cellular structure of black holes.** The event horizon corresponds to the outer nuclear membrane and the Cauchy horizon to the inner nuclear membrane; in the Schwarzschild case, which has no inner horizon, the inner nuclear membrane corresponds to the inner interface $R_i = R_s/2$; R_i depends only on the total energy, is the boundary confining the capsule packs, and applies equally to Kerr black holes. The sum of the entropies of the two horizons is $4\pi k_B N^2$, and the sum of the two horizon areas is always four times the area of the inner interface. The areal radius of the inner horizon crosses R_i at $\chi = \sqrt{3}/2$: $\chi < \sqrt{3}/2$ is the prokaryotic type and $\chi > \sqrt{3}/2$ the eukaryotic type, a division that coincides with Smarr's critical value for embedding the outer horizon [22]; a cosmic egg cell must be eukaryotic. The difference of the areal radii of the two horizons is not smaller than $2\ell_p$; a separation equal to $2\ell_p$ is the existence boundary, below which the structure breaks, and the classical extremal point at which the two horizons coincide cannot be reached [3, 4]. The outer-horizon entropy corresponds to surface information and the inner-horizon entropy to bulk information; in a Schwarzschild black hole the bulk has lost its structure, $S_- = 0$, and all information is registered on the outer horizon. The nucleus contains the E_c packs registered in packing order and their pairwise relations, and this set of relations is the organizational code of the black hole: N^2 is the registration capacity and K_N the concrete code.
5. **Our universe and the remnant of the parent black hole.** When the parent black hole burst, the registrations on its inner and outer horizons transferred together into the Hubble sphere of the parent universe (i.e. our universe), with initial radius $2N_b\ell_p$ and mean density ρ_c/N_b^2, while each pack itself is at ρ_c; thereafter the Hubble sphere grows with the universe and always lies at its own Schwarzschild radius. The generations of universes share the same E_c background, and any point has a single temperature. The remnant of the parent black hole and the imprint of the ancestral universe can still be seen in our universe. The burst criterion follows from the existence criterion for black holes: the last rotational pack takes the separation of the two horizons below $2\ell_p$ in one step, the registrations on the two horizons mix, and the structure breaks and bursts. At a black-hole burst registration is completed in one step, and the relations as a whole become the organizational code of the new universe; the conversion of matter follows a dynamical process and

recombines according to the code, and the debris near the throat persists for a long time.

6. **Dark energy, dark matter and visible matter.** E_c has only three evolutionary pathways: remaining free, i.e. the background shared by all generations (dark energy, $w = -1$); re-clustering into black holes (dark matter); and being unpacked into radiation that condenses into particles, atoms and celestial bodies (visible matter). What the burst distributes is only matter: the dark-matter part clusters preferentially at the highest density, and the rest is unpacked and dilutes uniformly with the expansion. Accretion within a generation slowly converts visible matter into dark matter, but the conversion is still small; today's ratio of dark matter to baryons of about 5.4 reflects the distribution at the burst together with possible cross-generational black holes, and can serve only as a reference.
7. **Implicate and explicate order.** In the course of black-hole evolution, the two are the internal and external readings of the same set of relations: "maximal black-hole entropy means maximal disorder" is the external reading, "all relations established means maximal order" the internal reading. The unfolding of the universe is the process by which the implicate order turns into the explicate order through the burst and recombination by code.
8. **Cross-scale isomorphism.** The three-in-one structure of cosmic viviparity (nourishment by the accretion disc), ovoviviparity (isolation by the horizon) and oviparity (the black-hole burst), transgenerational pre-setting, deconstruction and information storage, and the three-level response mechanisms are all isomorphic to the corresponding mechanisms in biological systems. The CMB axis of evil, the Cold Spot and supermassive black holes may form the observational clue of an ancestral–parent–child "three generations in one frame".

8.2 Limitations and open questions

Throughout, this paper uses a hypothetical and exploratory structural mapping, not a rigorous mathematical proof of the proposition that "the universe has a holographic structure". On the physical nature of dark matter, the clustering of primordial black holes, the theoretical status of Bohm's implicate order, and cosmic generations and the origin of CMB anomalies, the paper takes definite positions; these are choices made while acknowledging that genuine disagreement remains. The specific open questions are:

1. The burst criterion of black holes is given by the existence criterion (Section 4.3), but how a cosmic egg cell gets past the spin cutoff of accretion-disc radiation (about 0.998) [56] to reach the existence boundary, and the source of co-rotating angular momentum in the accretion flow, have not been given.
2. If all the matter within today's Hubble sphere came from the parent black hole, then $N_b \approx 1.3 \times 10^{60}$, whereas TON 618 has $N \approx 6.0 \times 10^{48}$, smaller by about 2×10^{11}; how a germ-line black hole grows to the burst point, or whether a new universe can start from a smaller N_b, requires dedicated discussion.
3. The ratio of dark to visible matter at the burst, and the duration of the rapid-creation stage and the fraction converted into radiation, are in this paper all

determined by the organizational code and not random; their values are expressed in the observed dark-matter-to-baryon ratio (about 5.4) and baryon-to-photon ratio (about 6×10^{-10}). This paper reads these values from observation and cannot yet derive them directly from the code.

4. The conclusion about black-hole cores inside celestial bodies depends on the premise that "dark matter consists of black holes" and on the mass spectrum of dark-matter black holes; Population III stars have not yet been observed directly.
5. The relation between the E_c background shared by all generations, with its own expansion rate, and the capsule creation-rate equation of Paper II is still preliminary.
6. How later-registered information influences the fine-tuning of the physical parameters of the child universe has no quantitative formulation at present.
7. The concrete physical encoding of the relational code q_{ij} and its state space have not been given.
8. "The Cold Spot is the debris of the parent black hole" is an independent claim that needs support from the particularity of the Cold Spot direction; the amplitude of the debris potential well must not exceed the observational limits on the large-scale isotropy of the CMB.
9. The concrete dynamics of the early stage of the burst have not been given: the release process after breaking, the transfer of the registrations on the two horizons into the Hubble sphere, how the preferentially released clustered matter and the unpacked radiation are distributed, how the throat jet mixes with the matter released as a whole and becomes isotropic on large scales to about 10^{-5}, and how the actual size of the throat opening changes.
10. The energy account of rapid creation, of the $1 + 1 \to 2 \to 1$ cycle and of radiation generation, including the fate of the negative gravitational energy in the zero sum of the background and its quantitative effect on the local expansion.
11. Whether the background shared by all generations and the inherited organizational code can remove the horizon problem of standard cosmology requires dedicated study.
12. Cross-generational energy balance. Most black holes in a universe stay in their own generation, and only very few reach the burst point and pass relations and matter on to the child generation, just as germ cells make up only a tiny fraction of the cells of an individual. We assume that each bursting black hole releases, according to the code, an amount of matter equal to what it has retained, divided by the code into dark and visible matter; every burst then balances, and the cross-generational balance raises no contradiction. Today's observed dark matter may include black holes from the parent or even earlier generations, in unknown proportion. We map the parent black hole only onto the Hubble sphere; which generation the matter beyond the Hubble sphere comes from, and how much there is, cannot be decided by temperature, since all generations share the same background and the same temperature, and we make no inference. How the universe balances energy between generations requires further understanding.

8.3 Outlook

Observational tests. (1) The equation of state of dark energy: if $w(z)$ is confirmed to deviate from -1, this will directly test the dark-energy picture of Paper II and of this paper. (2) Primordial black holes: detection in the asteroid-mass window, and statistics of black-hole cores in the remnants of Population III stars. (3) The CMB: whether the lensing signal in the direction of the Cold Spot is a mass excess (remnant and debris) or a mass deficit (supervoid); the frequency dependence of the Cold Spot core temperature (the remnant's shadow); the geometric correlation of the Cold Spot with the axis of evil and the north–south hemispherical power asymmetry; the hierarchy of scale and amplitude of the relics of the three generations; and whether the spin axes of supermassive black holes are biased towards the global principal axis (orientational order parameter $Q > 0$, Section 6.1). (4) Generational nesting: whether the overlapping region contains objects older than the local age of the universe; the prematurely mature massive galaxies discovered by JWST may be a clue, but this is still disputed. (5) Black-hole spin: by Section 2.5, merger products lie mostly in the prokaryotic region, black holes grown by accretion move gradually into the eukaryotic region, and candidates for cosmic egg cells should have spins above $\sqrt{3}/2$. Existing X-ray reflection-spectrum measurements suggest that black holes more massive than about $3 \times 10^7\, M_\odot$ have lower spins [24]; spin measurements of the most massive black holes of the TON 618 class will be a direct test.

Parallel universes. In the observable universe, black holes with masses of about $6.6 \times 10^{10} M_\odot$ like TON 618 are extremely rare, estimated to number in the hundreds to thousands. If the laws of physics are universal, all supermassive black holes reaching the critical scale have the potential to give birth to their own new universes; they need not burst at the same time but unfold one after another at their own spacetime nodes, forming local new universes causally isolated from one another. To us these new universes are "parallel" and do not interfere with one another; to the parent universe they are all the next generation born of the same mother. This idea is a speculative extension and is left for future work.

Acknowledgements. The author used Claude (Anthropic) to assist with language editing, translation, LaTeX typesetting and organization of the manuscript, and to help identify internal inconsistencies during revision; ChatGPT (OpenAI) was used for critical reading and consistency checking of the manuscript. All physical reasoning and the results reported here were conceived and directed by the author; all AI-assisted text, derivations and typesetting were reviewed and checked by the author, and corrected where necessary, before inclusion. No AI tool was used to carry out independent physical analysis or to generate scientific claims without the author's direction and verification.

Declarations

- **Funding.** This research received no specific funding.
- **Competing interests.** The author declares no competing interests.
- **Ethics approval and consent to participate.** Not applicable.
- **Consent for publication.** Not applicable.

- **Data availability.** This is a theoretical study; no new observational data were generated. The published observational parameters used are given in the cited references.
- **Materials availability.** Not applicable.
- **Code availability.** Not applicable.
- **Author contribution.** G. Gu is the sole author and is responsible for the conception, derivations, analysis and writing of this work.

References

[1] Gu, G.: Unified recursive organization theory: toward a general framework for biological holography. Zenodo preprint (2026). DOI:10.5281/zenodo.21972530

[2] Gu, G.: The $2d_m$ minimum topological structural unit: from the relational-information axiom to the dark-energy capsule and the cosmological residual potential. Zenodo preprint (2026). DOI:10.5281/zenodo.24182016

[3] Gu, G.: Relational structure of the Bekenstein–Hawking entropy: quantized accretion and evaporation, the Page curve and the entropy of Kerr black holes. Zenodo preprint (2026). DOI:10.5281/zenodo.24476341

[4] Gu, G.: Angular-momentum spectrum of Kerr black holes: basis of the existence criterion, spin evolution and breaking. Zenodo preprint (2026). DOI:10.5281/zenodo.24511425

[5] Bekenstein, J.D.: Black holes and entropy. Phys. Rev. D **7**(8), 2333–2346 (1973). DOI:10.1103/PhysRevD.7.2333

[6] 't Hooft, G.: Dimensional reduction in quantum gravity. arXiv:gr-qc/9310026 (1993)

[7] Susskind, L.: The world as a hologram. J. Math. Phys. **36**(11), 6377–6396 (1995). DOI:10.1063/1.531249

[8] Bousso, R.: The holographic principle. Rev. Mod. Phys. **74**(3), 825–874 (2002). DOI:10.1103/RevModPhys.74.825

[9] Smolin, L.: Did the universe evolve? Class. Quantum Grav. **9**(1), 173–191 (1992). DOI:10.1088/0264-9381/9/1/016

[10] Niikura, H., Takada, M., Yasuda, N., Lupton, R.H., Sumi, T., et al.: Microlensing constraints on primordial black holes with Subaru/HSC Andromeda observations. Nat. Astron. **3**(6), 524–534 (2019). DOI:10.1038/s41550-019-0723-1

[11] Carr, B., Kohri, K., Sendouda, Y., Yokoyama, J.: Constraints on primordial black holes. Rep. Prog. Phys. **84**(11), 116902 (2021). DOI:10.1088/1361-6633/ac1e31

[12] Adame, A.G., et al. (DESI Collaboration): DESI 2024 VI: cosmological constraints from the measurements of baryon acoustic oscillations. J. Cosmol. Astropart. Phys. **2025**(02), 021 (2025). DOI:10.1088/1475-7516/2025/02/021

[13] Calderon, R., Lodha, K., Shafieloo, A., Linder, E., et al. (DESI Collaboration): DESI 2024: reconstructing dark energy using crossing statistics with DR1 BAO data. J. Cosmol. Astropart. Phys. **2024**(10), 048 (2024). DOI:10.1088/1475-7516/2024/10/048

[14] García-Bellido, J., Clesse, S.: Constraints from microlensing experiments on clustered primordial black holes. Phys. Dark Universe **19**, 144–148 (2018). DOI:10.1016/j.dark.2018.01.001

[15] Jedamzik, K.: Consistency of primordial black hole dark matter with LIGO/Virgo merger rates. Phys. Rev. Lett. **126**, 051302 (2021). DOI:10.1103/PhysRevLett.126.051302

[16] De Luca, V., Desjacques, V., Franciolini, G., Riotto, A.: The clustering evolution of primordial black holes. J. Cosmol. Astropart. Phys. **2020**(11), 028 (2020). DOI:10.1088/1475-7516/2020/11/028

[17] De Luca, V., Franciolini, G., Riotto, A., Veermäe, H.: Ruling out initially clustered primordial black holes as dark matter. Phys. Rev. Lett. **129**(19), 191302 (2022). DOI:10.1103/PhysRevLett.129.191302

[18] Bohm, D.: Wholeness and the Implicate Order. Routledge, London (2005). Original work published 1980. DOI:10.4324/9780203995150

[19] Bohm, D., Hiley, B.J.: The Undivided Universe: An Ontological Interpretation of Quantum Theory. Routledge, London (1993; reprinted 2006). DOI:10.4324/9780203980385

[20] Schmieke, M.: Bohm's super implicate order and the quantum Zeno effect. Interdiscip. Int. J. **19**, 1–10 (2022). DOI:10.36018/dsiij.v19i.241

[21] Bekenstein, J.D.: Universal upper bound on the entropy-to-energy ratio for bounded systems. Phys. Rev. D **23**(2), 287–298 (1981). DOI:10.1103/PhysRevD.23.287

[22] Smarr, L.: Surface geometry of charged rotating black holes. Phys. Rev. D **7**(2), 289–295 (1973). DOI:10.1103/PhysRevD.7.289

[23] Abbott, R., et al. (LIGO Scientific Collaboration, Virgo Collaboration and KAGRA Collaboration): GWTC-3: compact binary coalescences observed by LIGO and Virgo during the second part of the third observing run. Phys. Rev. X **13**, 041039 (2023). DOI:10.1103/PhysRevX.13.041039

[24] Reynolds, C.S.: Observational constraints on black hole spin. Annu. Rev. Astron. Astrophys. **59**, 117–154 (2021). DOI:10.1146/annurev-astro-112420-035022

[25] Poisson, E., Israel, W.: Internal structure of black holes. Phys. Rev. D **41**(6), 1796–1809 (1990). DOI:10.1103/PhysRevD.41.1796

[26] Dafermos, M., Luk, J.: The interior of dynamical vacuum black holes I: the C^0-stability of the Kerr Cauchy horizon. Ann. Math. **202**(2), 309–630 (2025). DOI:10.4007/annals.2025.202.2.1

[27] Carr, B.J., Hawking, S.W.: Black holes in the early Universe. Mon. Not. R. Astron. Soc. **168**(2), 399–415 (1974). DOI:10.1093/mnras/168.2.399

[28] Carr, B.J.: The primordial black hole mass spectrum. Astrophys. J. **201**, 1–19 (1975). DOI:10.1086/153853

[29] Harada, T., Yoo, C.-M., Kohri, K.: Threshold of primordial black hole formation. Phys. Rev. D **88**, 084051 (2013). DOI:10.1103/PhysRevD.88.084051

[30] Custódio, P.S., Horvath, J.E.: Evolution of a primordial black hole population. Phys. Rev. D **58**, 023504 (1998). DOI:10.1103/PhysRevD.58.023504

[31] Carr, B.J., Kohri, K., Sendouda, Y., Yokoyama, J.: New cosmological constraints on primordial black holes. Phys. Rev. D **81**, 104019 (2010). DOI:10.1103/PhysRevD.81.104019

[32] Haque, M.R., Karmakar, R., Mambrini, Y.: When primordial black holes absorb during the early universe. arXiv:2601.16717 (2026). DOI:10.48550/arXiv.2601.16717

[33] Thanh, N.T.K., Maclean, N., Mahiddine, S.: Mechanisms of nucleation and growth of nanoparticles in solution. Chem. Rev. **114**(15), 7610–7630 (2014). DOI:10.1021/cr400544s

[34] Bambi, C., Spolyar, D., Dolgov, A.D., Freese, K., Volonteri, M.: Implications of primordial black holes on the first stars and the origin of the super-massive black holes. Mon. Not. R. Astron. Soc. **399**(3), 1347 (2009). DOI:10.1111/j.1365-2966.2009.15367.x

[35] Bellinger, E.P., Caplan, M.E., Ryu, T., Bollimpalli, D., Ball, W.H., Kühnel, F., Farmer, R., de Mink, S.E., Christensen-Dalsgaard, J.: Solar evolution models with a central black hole. Astrophys. J. **959**, 113 (2023). DOI:10.3847/1538-4357/ad04de

[36] Capela, F., Pshirkov, M., Tinyakov, P.: Constraints on primordial black holes as dark matter candidates from star formation. Phys. Rev. D **87**, 023507 (2013). DOI:10.1103/PhysRevD.87.023507

[37] Caplan, M.E., Bellinger, E.P., Santarelli, A.C.: Is there a black hole in the center of the Sun? Astrophys. Space Sci. **369**, 8 (2024). DOI:10.1007/s10509-024-04270-1

[38] Gottlieb, O., Cantiello, M., Norton, C., Van Tilburg, K., Kleban, M.: The life and death of stars that capture primordial black holes. arXiv:2606.02700 (2026). DOI:10.48550/arXiv.2606.02700

[39] Dai, D.-C., Stojkovic, D.: Searching for small primordial black holes in planets, asteroids and here on Earth. Phys. Dark Universe **46**, 101662 (2024). DOI:10.1016/j.dark.2024.101662

[40] Ballesteros, G., Taoso, M.: Primordial black hole dark matter from single field inflation. Phys. Rev. D **97**, 023501 (2018). DOI:10.1103/PhysRevD.97.023501

[41] Santarelli, A.D., Caplan, M.E., Smith, N.T.: Possible constraints on asteroid-mass primordial black holes from Solar System cratering. Mon. Not. R. Astron. Soc. **538**(1), 108–113 (2025). DOI:10.1093/mnras/staf300

[42] Montero-Camacho, P., Fang, X., Vasquez, G., Silva, M., Hirata, C.M.: Revisiting constraints on asteroid-mass primordial black holes as dark matter candidates. J. Cosmol. Astropart. Phys. **2019**(08), 031 (2019). DOI:10.1088/1475-7516/2019/08/031

[43] Desjacques, V., Riotto, A.: Spatial clustering of primordial black holes. Phys. Rev. D **98**, 123533 (2018). DOI:10.1103/PhysRevD.98.123533

[44] Pathria, R.K.: The universe as a black hole. Nature **240**, 298–299 (1972). DOI:10.1038/240298a0

[45] Good, I.J.: Chinese universes. Phys. Today **25**(7), 15 (1972). DOI:10.1063/1.3070923

[46] Smoller, J., Temple, B.: Shock-wave cosmology inside a black hole. Proc. Natl. Acad. Sci. USA **100**(20), 11216–11218 (2003). DOI:10.1073/pnas.1833875100

[47] Fixsen, D.J., Cheng, E.S., Gales, J.M., Mather, J.C., Shafer, R.A., Wright, E.L.: The cosmic microwave background spectrum from the full COBE FIRAS data set. Astrophys. J. **473**, 576–587 (1996). DOI:10.1086/178173

[48] Noterdaeme, P., Petitjean, P., Srianand, R., Ledoux, C., López, S.: The evolution of the cosmic microwave background temperature: measurements of $T_{\rm CMB}$ at high redshift from carbon monoxide excitation. Astron. Astrophys. **526**, L7 (2011). DOI:10.1051/0004-6361/201016140

[49] Sato, K.: First-order phase transition of a vacuum and expansion of the Universe. Mon. Not. R. Astron. Soc. **195**(3), 467–479 (1981).

DOI:10.1093/mnras/195.3.467

[50] Guth, A.H.: Inflationary universe: a possible solution to the horizon and flatness problems. Phys. Rev. D **23**(2), 347–356 (1981). DOI:10.1103/PhysRevD.23.347

[51] Linde, A.D.: A new inflationary universe scenario: a possible solution of the horizon, flatness, homogeneity, isotropy and primordial monopole problems. Phys. Lett. B **108**(6), 389–393 (1982). DOI:10.1016/0370-2693(82)91219-9

[52] Linde, A.D.: Chaotic inflation. Phys. Lett. B **129**(3–4), 177–181 (1983). DOI:10.1016/0370-2693(83)90837-7

[53] Parikh, M.K., Wilczek, F.: Hawking radiation as tunneling. Phys. Rev. Lett. **85**, 5042–5045 (2000). DOI:10.1103/PhysRevLett.85.5042

[54] Frolov, V.P., Markov, M.A., Mukhanov, V.F.: Through a black hole into a new universe? Phys. Lett. B **216**(3–4), 272–276 (1989). DOI:10.1016/0370-2693(89)91114-3

[55] Popławski, N.J.: Radial motion into an Einstein–Rosen bridge. Phys. Lett. B **687**(2–3), 110–113 (2010). DOI:10.1016/j.physletb.2010.03.029

[56] Thorne, K.S.: Disk-accretion onto a black hole. II. Evolution of the hole. Astrophys. J. **191**, 507–520 (1974). DOI:10.1086/152991

[57] Planck Collaboration, Aghanim, N., et al.: Planck 2018 results. VI. Cosmological parameters. Astron. Astrophys. **641**, A6 (2020). DOI:10.1051/0004-6361/201833910

[58] Marconi, A., Risaliti, G., Gilli, R., Hunt, L.K., Maiolino, R., Salvati, M.: Local supermassive black holes, relics of active galactic nuclei and the X-ray background. Mon. Not. R. Astron. Soc. **351**, 169–185 (2004). DOI:10.1111/j.1365-2966.2004.07765.x

[59] Fukugita, M., Peebles, P.J.E.: The cosmic energy inventory. Astrophys. J. **616**(2), 643–668 (2004). DOI:10.1086/425155

[60] Babichev, E., Dokuchaev, V., Eroshenko, Yu.: Black hole mass decreasing due to phantom energy accretion. Phys. Rev. Lett. **93**, 021102 (2004). DOI:10.1103/PhysRevLett.93.021102

[61] van de Weygaert, R.: Voids and the cosmic web: cosmic depressions & spatial complexity. Proc. Int. Astron. Union **11**(S308), 493–523 (2016). DOI:10.1017/S1743921316010504

[62] Lohrey, A., Boreham, B.: Lifting the veil on Bohm's holomovement. Commun. Integr. Biol. **14**(1), 221–229 (2021). DOI:10.1080/19420889.2021.2001157

[63] Torday, J.S.: Evolution, gravity, and the topology of consciousness. Prog. Biophys. Mol. Biol. **174**, 50–54 (2022). DOI:10.1016/j.pbiomolbio.2022.06.005

[64] Brillouin, L.: The negentropy principle of information. J. Appl. Phys. **24**(9), 1152–1163 (1953). DOI:10.1063/1.1721463

[65] Parrondo, J.M.R., Horowitz, J.M., Sagawa, T.: Thermodynamics of information. Nat. Phys. **11**(2), 131–139 (2015). DOI:10.1038/nphys3230

[66] Planck Collaboration: Planck 2015 results. XVI. Isotropy and statistics of the CMB. Astron. Astrophys. **594**, A16 (2016). DOI:10.1051/0004-6361/201526681

[67] Land, K., Magueijo, J.: Examination of evidence for a preferred axis in the cosmic radiation anisotropy. Phys. Rev. Lett. **95**(7), 071301 (2005). DOI:10.1103/PhysRevLett.95.071301

[68] de Oliveira-Costa, A., Tegmark, M., Zaldarriaga, M., Hamilton, A.: The significance of the largest scale CMB fluctuations in WMAP. Phys. Rev. D **69**(6), 063516 (2004). DOI:10.1103/PhysRevD.69.063516

[69] Planck Collaboration, Aghanim, N., et al.: Planck 2018 results. I. Overview and the cosmological legacy of Planck. Astron. Astrophys. **641**, A1 (2020). DOI:10.1051/0004-6361/201833880

[70] de Gennes, P.G., Prost, J.: The Physics of Liquid Crystals, 2nd edn. Clarendon Press, Oxford (1993)

[71] Hutsemékers, D.: Evidence for very large-scale coherent orientations of quasar polarization vectors. Astron. Astrophys. **332**, 410–428 (1998)

[72] Hutsemékers, D., Cabanac, R., Lamy, H., Sluse, D.: Mapping extreme-scale alignments of quasar polarization vectors. Astron. Astrophys. **441**, 915–930 (2005). DOI:10.1051/0004-6361:20053337

[73] Taylor, A.R., Jagannathan, P.: Alignments of radio galaxies in deep radio imaging of ELAIS N1. Mon. Not. R. Astron. Soc. **459** (2016). arXiv:1603.02418

[74] Cruz, M., Martínez-González, E., Vielva, P., Cayón, L.: Detection of a non-Gaussian spot in WMAP. Mon. Not. R. Astron. Soc. **356**(1), 29–40 (2005). DOI:10.1111/j.1365-2966.2004.08419.x

[75] Cruz, M., Tucci, M., Martínez-González, E., Vielva, P.: The non-Gaussian cold spot in Wilkinson Microwave Anisotropy Probe: significance, morphology and foreground contribution. Mon. Not. R. Astron. Soc. **369**(1), 57–67 (2006). DOI:10.1111/j.1365-2966.2006.10312.x

[76] Cruz, M., Cayón, L., Martínez-González, E., Vielva, P., Jin, J.: The non-Gaussian cold spot in the 3 year Wilkinson Microwave Anisotropy Probe data. Astrophys.

J. **655**(1), 11–20 (2007). DOI:10.1086/509703

[77] Cruz, M., Martínez-González, E., Vielva, P., Diego, J.M., Hobson, M., Turok, N.: The CMB cold spot: texture, cluster or void? Mon. Not. R. Astron. Soc. **390**(3), 913–919 (2008). DOI:10.1111/j.1365-2966.2008.13812.x

[78] Szapudi, I., Kovács, A., Granett, B.R., Frei, Z., Silk, J., et al.: Detection of a supervoid aligned with the cold spot of the cosmic microwave background. Mon. Not. R. Astron. Soc. **450**(1), 288–294 (2015). DOI:10.1093/mnras/stv488

[79] An, D., Meissner, K.A., Nurowski, P., Penrose, R.: Apparent evidence for Hawking points in the CMB sky. Mon. Not. R. Astron. Soc. **495**(3), 3403–3408 (2020). DOI:10.1093/mnras/staa1343

[80] Jow, D.L., Scott, D.: Re-evaluating evidence for Hawking points in the CMB. J. Cosmol. Astropart. Phys. **2020**(03), 021 (2020). DOI:10.1088/1475-7516/2020/03/021

[81] Juodžbalis, I., Marconcini, C., D'Eugenio, F., et al.: A direct black-hole mass measurement in a little red dot at high redshift. Nature **653**, 1017–1021 (2026). DOI:10.1038/s41586-026-10579-4

[82] Inayoshi, K., Ho, L.C.: A critical evaluation of the physical nature of the little red dots. Nature Astronomy **10**, 1261–1272 (2026). DOI:10.1038/s41550-026-02934-2

[83] Übler, H.: Massive black holes in the first billion years with JWST. Nature Astronomy **10**, 1273–1282 (2026). DOI:10.1038/s41550-026-02966-8

[84] Su, S.-C., Chu, M.-C.: Is the universe rotating? Astrophys. J. **703**, 354–361 (2009). DOI:10.1088/0004-637X/703/1/354

[85] Brensinger, S., Heitritter, K., Rodgers, V.G.J., Stiffler, K., Whiting, C.A.: Dark energy from dynamical projective connections. Class. Quantum Grav. **37**(5), 055003 (2020). DOI:10.1088/1361-6382/ab685d

[86] Shamir, L.: Analysis of $\sim 10^6$ spiral galaxies from four telescopes shows large-scale patterns of asymmetry in galaxy spin directions. Adv. Astron. **2022**, 8462363 (2022). DOI:10.1155/2022/8462363

[87] Shamir, L.: The distribution of galaxy rotation in JWST Advanced Deep Extragalactic Survey. Mon. Not. R. Astron. Soc. **538**(1), 76–91 (2025). DOI:10.1093/mnras/staf292

[88] Stringer, J.M., Barrand, S., Western, P.: Fine-tuning evolution: germline epigenetics and inheritance. Reproduction **146**(1), R37–R48 (2013). DOI:10.1530/REP-12-0526